RADAR FOLIAGE PENETRATION MEASUREMENTS AT
MILLIMETER WAVELENGTHS

GEORGIA INSTITUTE OF TECHNOLOGY

PREPARED FOR
FRANKFORT ARSENAL

31 DECEMBER 1975

REPORT DOCUMENTATION PAGE		READ INSTRUCTIONS BEFORE COMPLETING FORM
1. REPORT NUMBER	2. GOVT ACCESSION NO.	3. RECIPIENT'S CATALOG NUMBER
4. TITLE *(and Subtitle)* Radar Foliage Penetration Measurements at Millimeter Wavelengths		5. TYPE OF REPORT & PERIOD COVERED Final Technical Report 6/30/75 - 12/31/75
		6. PERFORMING ORG. REPORT NUMBER EES/GIT-A-1485-TR-4
7. AUTHOR(s) N. C. Currie, E. E. Martin, and F. B. Dyer		8. CONTRACT OR GRANT NUMBER(s) DAAA25-73-C-0256 Mod. P00006
9. PERFORMING ORGANIZATION NAME AND ADDRESS Engineering Experiment Station Georgia Institute of Technology Atlanta, Georgia 30332		10. PROGRAM ELEMENT, PROJECT, TASK AREA & WORK UNIT NUMBERS
11. CONTROLLING OFFICE NAME AND ADDRESS Frankford Arsenal United States Army Philadelphia, Pennsylvania 19137		12. REPORT DATE 31 December 1975
		13. NUMBER OF PAGES vii + 64
14. MONITORING AGENCY NAME & ADDRESS(if different from Controlling Office)		15. SECURITY CLASS. (of this report) Unclassified
		15a. DECLASSIFICATION/DOWNGRADING SCHEDULE N/A

16. DISTRIBUTION STATEMENT *(of this Report)*

The distribution of this report is unrestricted.

17. DISTRIBUTION STATEMENT *(of the abstract entered in Block 20, if different from Report)*

18. SUPPLEMENTARY NOTES

Georgia Tech Project A-1485-100

19. KEY WORDS *(Continue on reverse side if necessary and identify by block number)*

Radar	Polarization Properties	Vegetation
Penetration	Spectrum	Trees
Foliage	Millimeter Wave	Attenuation Coefficient
Propagation	Attenuation	

20. ABSTRACT *(Continue on reverse side if necessary and identify by block number)*

A series of radar measurements on the penetration of foliage have been made at 9.4, 16.2, 35, and 95 GHz. Measurements were made for both the one-way and two-way cases at 9.4 and 16.4 GHz at similar foliage areas for comparison. The bulk of the measurements were made at depression angles below 3°, although a set of one-way measurements were made at 9.4 and 16.2 GHz for a depression angle of 29°. Attenuation properties, polarization ratios, and noncoherent spectral and correlation properties were investigated as a function

DD $_{1\ JAN\ 73}^{FORM}$ 1473   EDITION OF 1 NOV 65 IS OBSOLETE   Unclassified
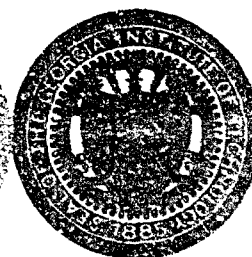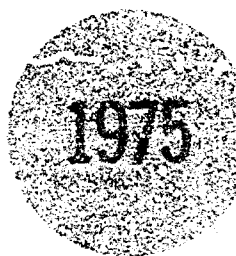
126104

TECHNICAL REPORT NO. 4

RADAR FOLIAGE PENETRATION MEASUREMENTS AT MILLIMETER WAVELENGTHS

FINAL REPORT ON
EES/GIT PROJECT A-1485-100

Prepared for

UNITED STATES ARMY
FRANKFORD ARSENAL
PHILADELPHIA, PA. 19137
        UNDER
CONTRACT DAAA 25-73-C-0256
        MOD. P00006

By

N. C. Currie, E. E. Martin, and F. B. Dyer

31 December 1975

ENGINEERING EXPERIMENT STATION
Georgia Institute of Technology
Atlanta, Georgia 30332

D D C

APR 30 1976

E

ENGINEERING EXPERIMENT STATION
Georgia Institute of Technology
Atlanta, Georgia   30332

RADAR FOLIAGE PENETRATION MEASUREMENTS AT
MILLIMETER WAVELENGTHS

Technical Report No. 4
EES/GIT Project A-1485

by

N. C. Currie, E. E. Martin, and F. B. Dyer

Prepared for

United States Army
Frankford Arsenal
Philadelphia, Pennsylvania   19137

FINAL REPORT
on
Contract DAAA 25-73-C-0256, Mod. P00006

31 December 1975

RADAR FOLIAGE PENETRATION MEASUREMENTS AT
MILLIMETER WAVELENGTHS

by

N. C. Currie, E. E. Martin, and F. B. Dyer

ABSTRACT

A series of radar measurements on the penetration of foliage has
been made at frequencies of 9.4, 16.2, 35, and 95 GHz. Comparison measure-
ments were made using both one-way and two-way techniques at 9.4 and
16.4 GHz, and two-way techniques only at 35 and 95 GHz for similar foliage
areas. The bulk of the measurements were made at depression angles below
3°, although a few one-way measurements were made at 9.4 and 16.2 GHz for
depression angles near 30°. Attenuation properties, polarization ratios,
and noncoherent spectral and correlation properties were investigated
as a function of frequency, polarization, depth of foliage, and wind
speed. Limited comparisons are made with published data for the lower
frequencies.

ACKNOWLEDGEMENTS

TABLE OF CONTENTS

LIST OF FIGURES

List of Figures (continued)

LIST OF TABLES

I. INTRODUCTION

This report summarizes the results of a measurement program to determine the characteristics of radar penetration of foliage at millimeter wavelengths which was conducted at Kennesaw National Battlefield Monument, Georgia, over the period August and September, 1975. Emphasis in the report is placed on determining the one-way and two-way attenuation properties of tree canopies for summer foliage conditions.

A. Background

The present program resulted from a need for information on the foliage penetration properties of radar signals in the region above 10 GHz which was identified by the Lincoln Laboratories, Massachusetts Institute of Technology. The work was intended to aid in the selection of the proper frequency band for a radar to be used in the mini-remotely-piloted-vehicle (mini-RPV) presently under development by the U.S. Army. The Engineering Experiment Station (EES) at Georgia Tech was selected to conduct the measurement program because of its expertise in the making of measurements in this frequency region as demonstrated by an on-going program for the Frankford Arsenal, U.S. Army under Contract DAAA-25-73-C-0256. The present measurement program was funded through Frankford Arsenal as an addition to Contract DAAA25-73-C-0256.

Previous work under this contract includes several complementary test programs in the millimeter region. A literature search to locate the available land clutter data above 1 GHz was conducted under the original contract, and the results were summarized with some limited modeling of the data in Technical Report No. 1. [1] Next, a test program was conducted jointly with the Ballistic Research Laboratories (BRL), Aberdeen, Maryland, to determine the radar backscatter properties of rain in the region 10 GHz to 100 GHz; the results of those tests are summarized in Technical Report No. 2. [2] Finally, a program to measure the backscatter properties from land clutter in the millimeter region for summer foliage conditions was conducted by EES for Frankford Arsenal; the results are summarized in Technical Report No. 3. [3] Further work in the millimeter region is planned on the contract in the near future, including a winter foliage penetration study and winter backscatter measurements.

B. Description of Field Measurements

The goals of this program were to make simultaneous measurements of the attenuation constants for forest type foliage at frequencies of 9.4, 16.2, 35, and 95 GHz, and if possible to gain an insight into the mechanisms which influence the attenuation. Three basic criteria had to be met to achieve these goals. First, a field site had to be selected which would allow a good-and-repeatable definition of foliage depth to be developed. Second, precision instrumentation and data acquisition equipment had to be used to obtain repeatable results. And third, proper test procedures had to be defined so that the winter penetration measurements, to be conducted in Phase II of the program, could be compared with the Phase I summer measurements. The discussions which follow will show how these criteria were met and hopefully will facilitate the use of the data obtained here for other problem areas. Particularly important are the discussions of the definition of foliage depth and the use of two independent measurement techniques to gather the attenuation data.

A two-way experiment was conducted by measuring the attenuation of a radar signal caused by foliage in front of a trihedral corner reflector. the reflector was in a clear unobstructed area and comparing that level to the level of video recorded when the corner was in an area where the radar view was obstructed by intervening foliage. The difference in the two video levels represented the total two-way attenuation. The corner reflector was first positioned in a clear area, then moved back into the foliage, in approximately 1 meter increments, until the return from the corner could not be distinguished from the normal clutter returns. The large radar returns from the foliage obscured returns from the corner reflector very quickly, so that this method did not allow deep penetrations into the wooded areas.

The one-way experiments provided much deeper penetration into foliage for two reasons. First, since only one path was involved, the attenuation was only half the two-way attenuation. Second, there was no radar return from the foliage to mask the desired received signal as in the two-way case. The one-way experiments were conducted in a manner similar to the two-way measurements except that the corner reflector was replaced by standard

gain horns and remote short-pulse transmitters operating at frequencies of 9.4 and 16.2 GHz. Equipment was not readily available to implement the one-way experiment at the higher frequencies so that one-way experiments were not performed at 35 GHz and 95 GHz.

1. Field Site

The locations of the field sites for these measurements were selected after careful investigation of several factors. Boresite declination angle, accessibility for transporting equipment into foliage areas, accessibility for accurately defining total path length and foliage penetration path length, and density and type of trees available were all factors to be considered. Two sites were selected which met the accessibility requirements and offered a variety of foliage types, including both deciduous and coniferous trees. Measurements at depression angles of up to 2 degrees were achievable at Site 1 while a depression angle of 0.4 degree was available at Site 2. A third site located on the campus of the Georgia Institute of Technology was selected which allowed measurements of a single oak tree at depression angles near 29 degrees. An aerial view of Site 1 is shown in Figure 1. This site is located in the Kennesaw National Battlefield Park. Site 2, also located in the park, was located 1/2 mile northeast of Site 1. The topography of these sites allowed measurements to be conducted in an environment free of multipath effects above a height of 3 meters.

Trees located around Site 1 are typical of forests in North Georgia. Foliage attenuation was measured at five locations around this site. Trees which make up this forest are of the deciduous type and consist primarily of oak, dogwood, hickory, sweetgum and maple. The height of the trees ranged from 4.5 to 21 meters; the smaller trees generally being located near the edges. Figure 2 is a photograph of one of the measurement locations. The distance from the radar van to foliage areas was between 150 and 300 meters. The radars were positioned at the highest point within the field and overlooked an area covered with grass from 10 to 70 cm high. The land sloped down from the position of the radars in three directions with the lowest point being approximately 10 meters below the radar antennas.

Site 2 was near an area containing a grove of young pine trees ranging in height from 3.5 to 8 meters. The largest tree trunk diameter within this pine grove was 19 cm, and the average trunk diameter (within the path of the deepest penetration measurement) was 11 cm. The average tree foliage

3

Figure 1.   Aerial view of Test Site 1 showing radar van
            and surrounding foliage areas.
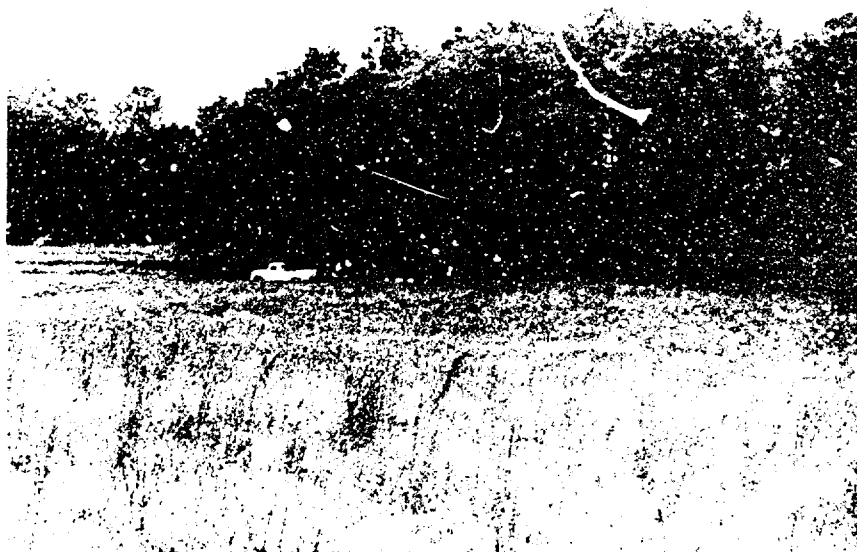
Figure 2.   Photograph of typical deciduous tree area
            near Test Site 1.

diameter (total) over this same path was 3 meters. Figure 3 shows this
young pine area. The radar van was positioned 160 meters from the pine
grove in a hay field which had been cut to a height of 7 cm about 3 weeks
earlier. The land around the van location was nearly flat for approximately
50 meters, and then very gently sloped down towards the pine grove. Data
were also collected on deciduous trees at this site.

Site 3 was located on the Georgia Tech campus. This site was selected
because of the large look angle which was available, and because it offered
an opportunity to observe a single oak tree and the possibility to repeat
the measurements with the tree in a defoliated state during Phase II of
the program. Because of the geometry of this site, only one-way attenuation
measurements were possible. Figure 4 is a view of the oak tree and the
building from which the measurements were made. The measurements were
conducted on a weekend to avoid the possible multipath effects caused by
parked automobiles. Transmitting equipment was located on the roof of
the building at a distance of 47 meters from the radar van. The geometry
of this site is shown in Figure 5. The radar van was moved laterally along
a straight line from a clear reference point to 8 different positions behind
the tree. The received signal levels were recorded at each position.
Attenuation coefficients were calculated for both horizontally and vertically
polarized transmitted signals.

2. Description of Test Equipment

a. Instrumentation Radars

The four instrumentation radars used for these measurements are mounted
in a single test vehicle along with integrated controls and data-acquisition
equipment, as shown in Figure 6. The 9 GHz, 16 GHz, and 35 GHz radars
are permanently mounted in the test vehicle with removable antennas on
the roof. To minimize waveguide losses, the 95 GHz radar is integrated
into a single package and sits on a platform on the van roof. The boresight
angle of each antenna is capable of being individually positioned in both
the azimuth and elevation planes. Parameters of the radars are given in
Tables 1 through 4. Although the I-Band and J-Band systems can be tuned
over a range of frequencies, they were set for these tests at 9.4 and 16.2
GHz, respectively.

Figure 3. Photograph of young pine grove at Test Site 2.

Figure 4. Photograph of oak tree at Test Site 3.

Tree Dimensions

Height ――――――――――― 17.3 m
Trunk Diameter ―――――― 0.75 m
Foliage Diameter ――――― 19.0 m
Height to Lowest Branch ― 3.5 m
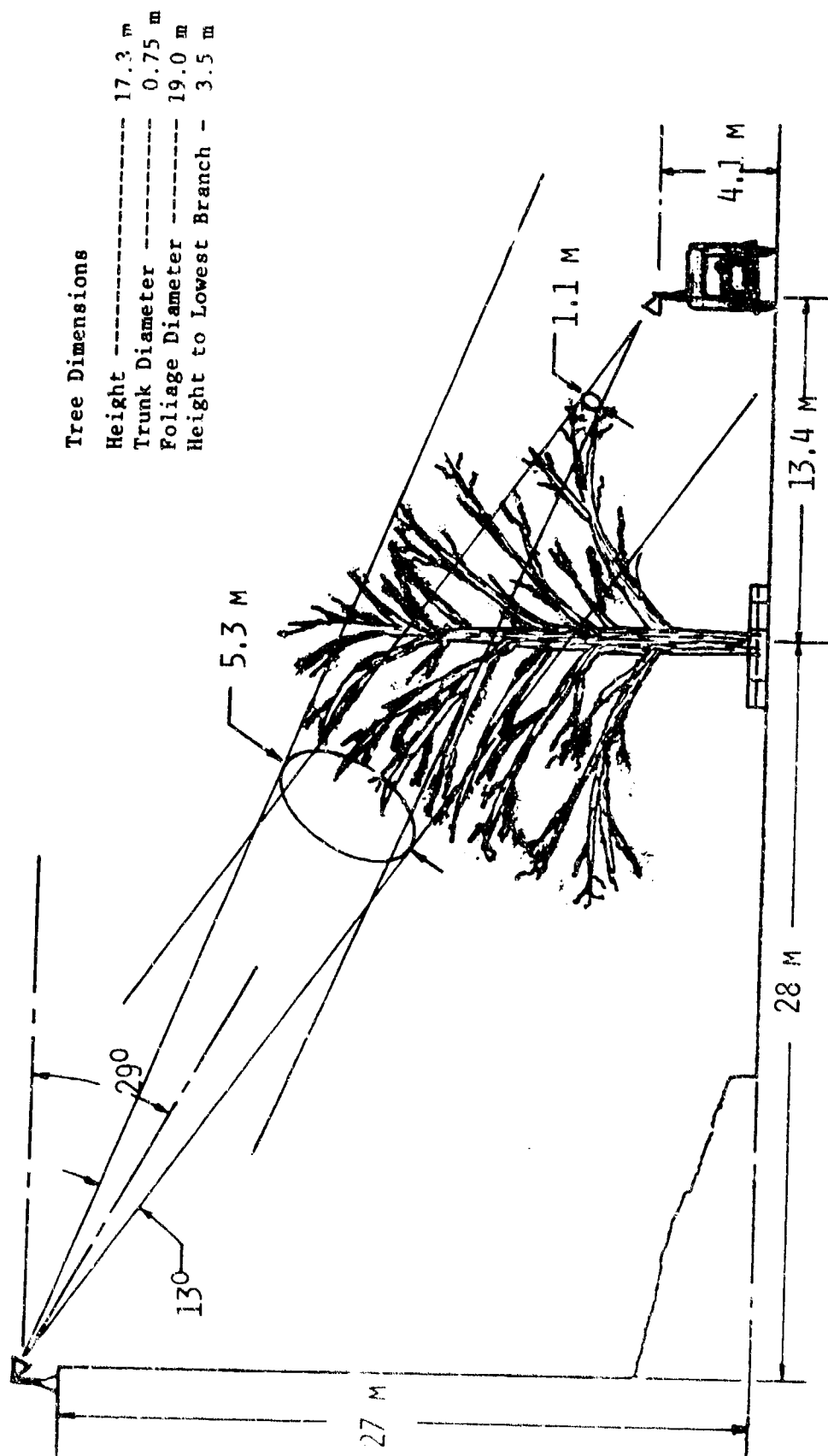
Figure 5. Geometry of one-way large depression angle experiment.

7
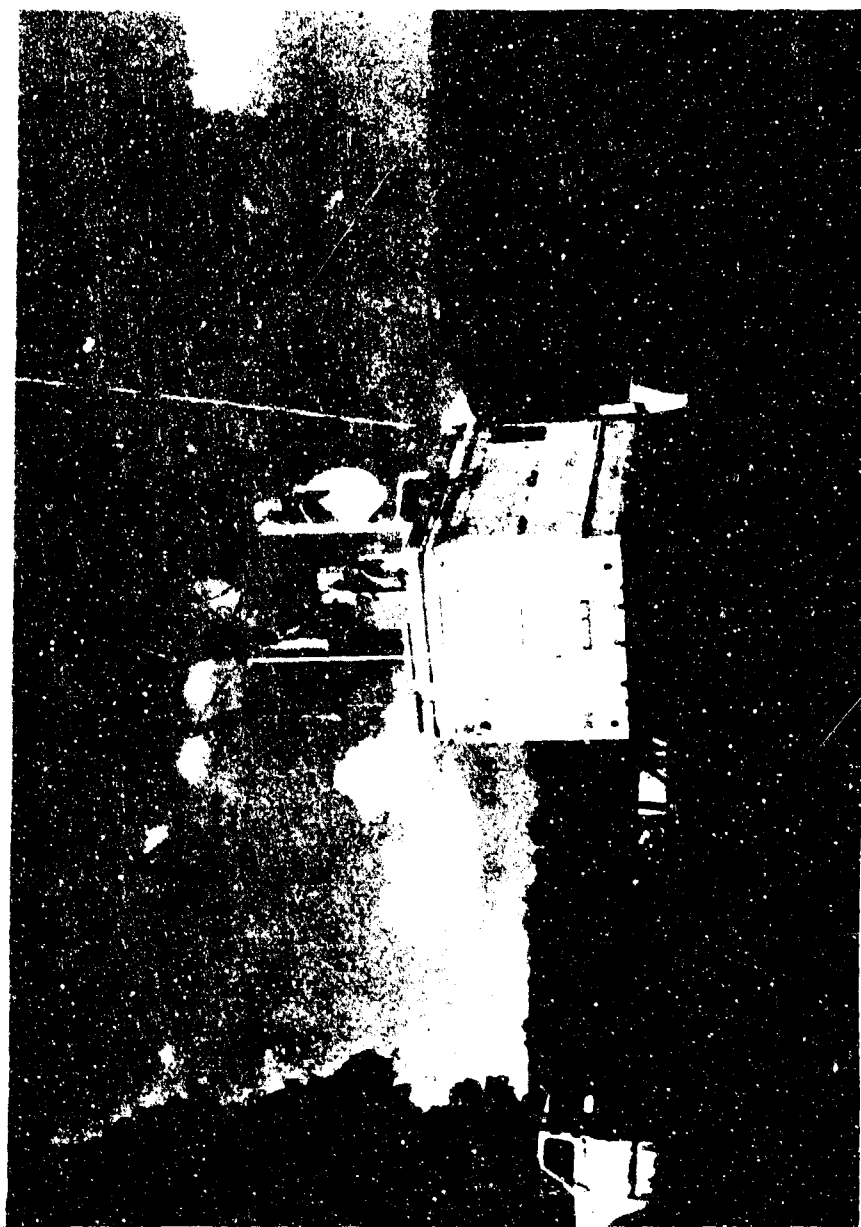
Figure 6. Photograph of test radar van located at Test Site 1.

TABLE 1

PARAMETERS OF GEORGIA TECH GT-I EXPERIMENTAL RADAR

Parameter	Description
Frequency	8.5-9.6 GHz
Peak Power	40 kW
Pulse Width	50 ns
PRF	0-4000 pps
Antenna Type	Nonscanning Paraboloid
Azimuth Beamwidth	1.5°
Elevation Beamwidth	1.65°
Antenna Gain	Vertical Polarization 41.4 dB
	Horizontal Polarization 41.6 dB
Antenna Type	Scanning Parabolic Cylinder
Scan Rate	0-100 RPM
Azimuth Beamwidth	2°
Elevation Beamwidth	5°
Antenna Gain	Vertical Polarization 30 dB
	Horizontal Polarization 31 dB
Polarization	H or V transmitted
	H and V received simultaneously
IF Center Frequency	60 MHz
IF Bandwidth	20 MHz
IF Response	Logarithmic (linear available)
Noise Figure	12 dB
Dynamic Range	80 dB
Display Type	A-scope

9

TABLE 2

PARAMETERS OF GEORGIA TECH GT-J EXPERIMENTAL RADAR

Parameter	Description
Frequency	16-17 GHz
Peak Power	50 kW
Pulse Width	50 ns
PRF	0-4000 pps
Antenna Type	Scanning Paraboloid
Scan Rate	0-120 rpm
Azimuth Beamwidth	1.5°
Elevation Beamwidth	1.5°
Antenna Gain	Vertical Polarization 41.5 dB
	Horizontal Polarization 41.4 dB
Polarization	H or V transmitted
	H and V received simultaneously
IF Center Frequency	60 MHz
IF Bandwidth	2C MHz
IF Response	Logarithmic (linear available)
Noise Figure	13 dB
Dynamic Range	70 dB
Display Type	A-scope, B-scope, PPI

TABLE 3

PARAMETERS OF GEORGIA TECH GT-K EXPERIMENTAL RADAR

Parameter	Description
Frequency	35 GHz
Peak Power	40 kW
Pulse Width	50 ns
PRF	0-4000 pps
Antenna Type	Scanning Paraboloid
Scan Rate	0-120 rpm
Azimuth Beamwidth	1°
Elevation Beamwidth	1°
Antenna Gain	Vertical Polarization 43 dB
	Horizontal Polarization 43 dB
Polarization	H or V transmitted
	H and H received simultaneously
IF Center Frequency	60 MHz
IF Bandwidth	20 MHz
IF Response	Logarithmic (linear available)
Noise Figure	14 dB
Dynamic Range	70 dB
Display Type	A-scope, B-scope, PPI

Table 4

PARAMETERS OF GEORGIA TECH GT-M EXPERIMENTAL RADAR

Parameter	Description
Frequency	95 GHz (Nom)
Peak Power	6 kW
Pulse Width	50 ns or 10 ns
PRF	0-4000 pps
Antenna Type	Paraboloid (Cassegrain)
Azimuth Beamwidth	.70°
Elevation Beamwidth	.65°
Antenna Gain	Vertical Polarization 46.3 dB
	Horizontal Polarization 46.3 dB
Polarization	H or V
IF Center Frequency	60 MHz or 160 MHz
IF Bandwidth	20 MHz or 100 MHz
IF Response	Logarithmic (linear available)
Noise Figure	15 dB
Dynamic Range	70 dB
Display Type	A-scope

While differing in detail, the 9, 16, and 35 GHz radars are generally similar. They are all short-pulse systems with dual-polarized antenna feeds; that is, they receive both horizontal and vertical polarizations simultaneously while transmitting either horizontal or vertical polarization. These three systems may be operated in either the scanning or non-scanning mode. The 9 GHz radar has both a 3-foot scanning parabolic cylinder and a 5-foot diameter nonscanning paraboloidal dish. Each antenna is equipped with boresight telescopes rigidly mounted to the antenna feed support. All three of these systems incorporate logarithmic receivers of wide dynamic range (approximately 80 dB) to permit accurate measurement of returns from targets having a widely varying signal strength. Each system incorporates provisions for injecting a known calibration signal into both parallel- and cross-polarized channels. A common prf reference of 2000 Hz was used for all systems during the tests described here. A simplified block diagram, typical of the radars used for these measurements is shown in Figure 7.

The 95 GHz system is somewhat different from the other three systems in that the antenna is a nonscanning Cassegrain type and all controls are mounted in one package containing antenna, transmitter, and receiver. A boresight telescope is also provided for accurately positioning the antenna. Although the antenna has a dual-polarized feed, only one receiver channel is currently incorporated.

The antenna sizes of the four radars resulted in beamwidths ranging between 1.5 degrees for the 9.5 GHz radar (2.0 degrees with the scanning parabolic cylinder) to 0.7 degrees for the 95 GHz radar. Figure 8 gives a close-up view of the four antennas on the top of the radar van.

b.   Remote Transmitters

To accomplish the one-way attenuation measurements, signal sources were required at the remote (target) site to transmit short pulses of energy to the receivers located in the radar van. These signals were provided by two low-power radar transmitters operating at 9.4 and 16.2 GHz, respectively. Parameters for the remote transmitters are given in Table 5. Synchronization between the remote equipment and the data-acquisition equipment was achieved by transmitting a short pulse at 9 GHz from the radar van. This pulse was detected, amplified and used to generate a

13
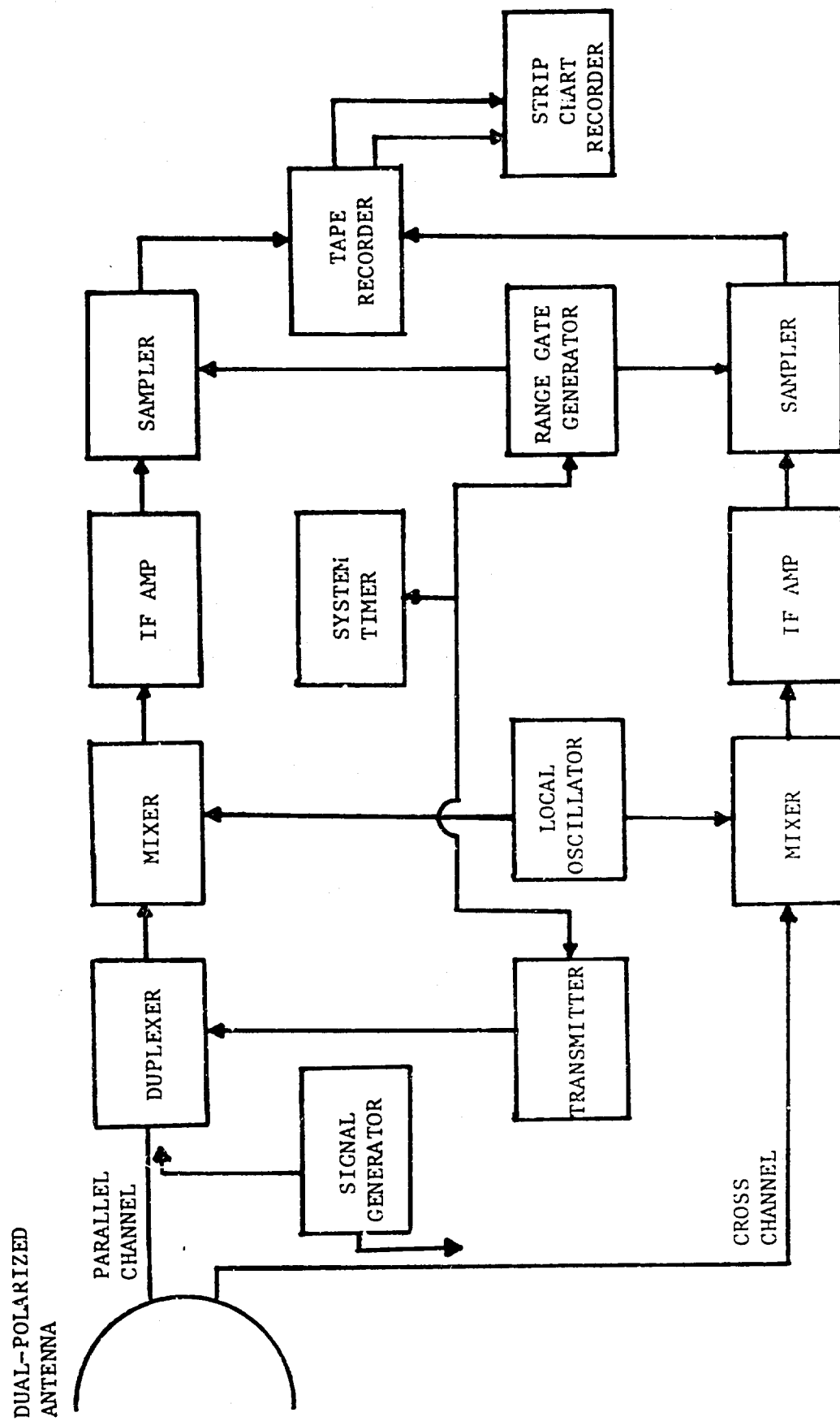
Figure 7. Simplified block diagram of equipment configuration of typical instrumentation radar.

14
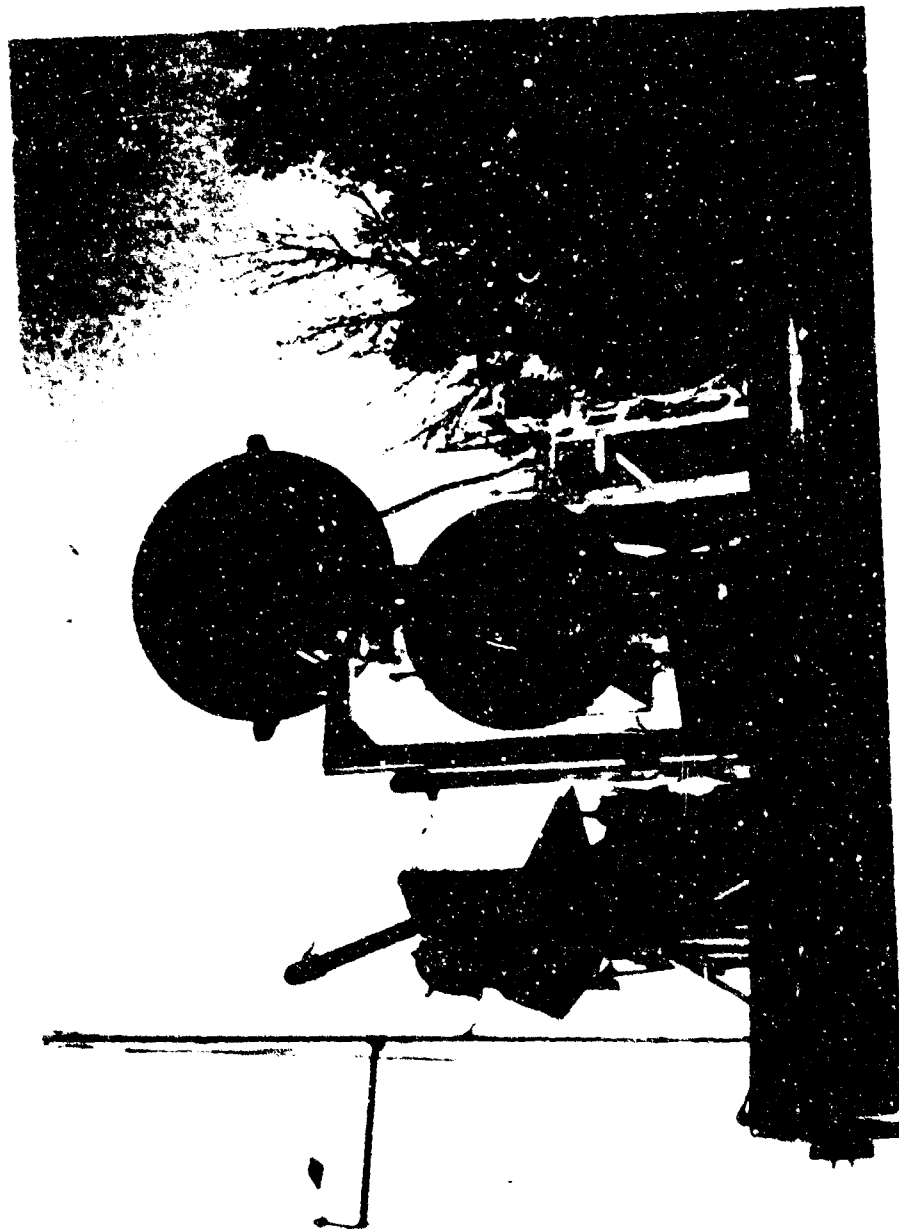
Figure 8. Close up view of radar antennas.

TABLE 5

PARAMETERS FOR REMOTE TRANSMITTERS

Parameter	Description	
Type	Pulsed Magnetron	
Modulator	Lumped Constant Delayline/Thyratron	
Frequency	9.4 GHz	16.2 GHz
Pulse Width	50 nsec	80 nsec
Peak Power	8 kW	8 kW
PRF	2000 Hz	2000 Hz
Antenna	SGH-8.20	SGH-12.4

trigger for the two remote transmitters. A block diagram of the equipment configuration used in the one-way measurements is shown in Figure 9. Signals from the remote locations were transmitted to the radar van through standard gain horns.

A photograph of the remote transmitters and synchronizing equipment used in the one-way attenuation measurements is shown in Figure 10.

c. Signal Conditioning and Recording Equipment

The rf energy received by the radar antennas is converted to an intermediate frequency in balanced mixers fed with local oscillators operating at frequencies 60 MHz below the received signal. The 60 MHz if signals are amplified and detected in RHG type LST 6026 logarithmic amplifiers. The resultant log video is buffered by line drivers before being routed to the various signal conditioning and monitoring equipment. Dual-mode couplers are incorporated into each antenna so that the two polarization components, one parallel to and one orthogonal to the polarization of the transmitted wave, are received. The two polarization components of the received signals are simultaneously processed through independent receiver channels for the 9, 16, and 35 GHz radars. (The 95 GHz radar is not presently configured for dual polarization.)

A console inside the radar van provides the operator easy access to the radar controls, displays, and data-acquisition equipment. A view of the radar console is shown in Figure 11. Located at the console are two A-scope displays, a B-scope display, a frequency counter and radar timing circuitry, and a six-channel narrow-aperture video sampler. The video sampler is used to sample, with a 30 nanosecond aperture, at a given range, the radar video from each of the six channels and hold the sampled value for one interpulse period. Amplitude data at the output of the video samplers are recorded on a 7-channel fm tape recorder with a dynamic range of approximately 40 dB. Typically four channels of the range gated and stretched video are recorded simultaneously along with a voice track, a sample synch pulse, and a time code signal. This allows the parallel channels at all four frequencies to be recorded simultaneously or parallel and cross channels at two frequencies to be recorded simultaneously.

The radar transmitter controls and rf signal generators are located in a rack to the left of the operator's console, as shown in Figure 12. The signal generators are used to calibrate the 9, 16, and 35 GHz radar receivers by injecting known rf signal levels into directional couplers

17
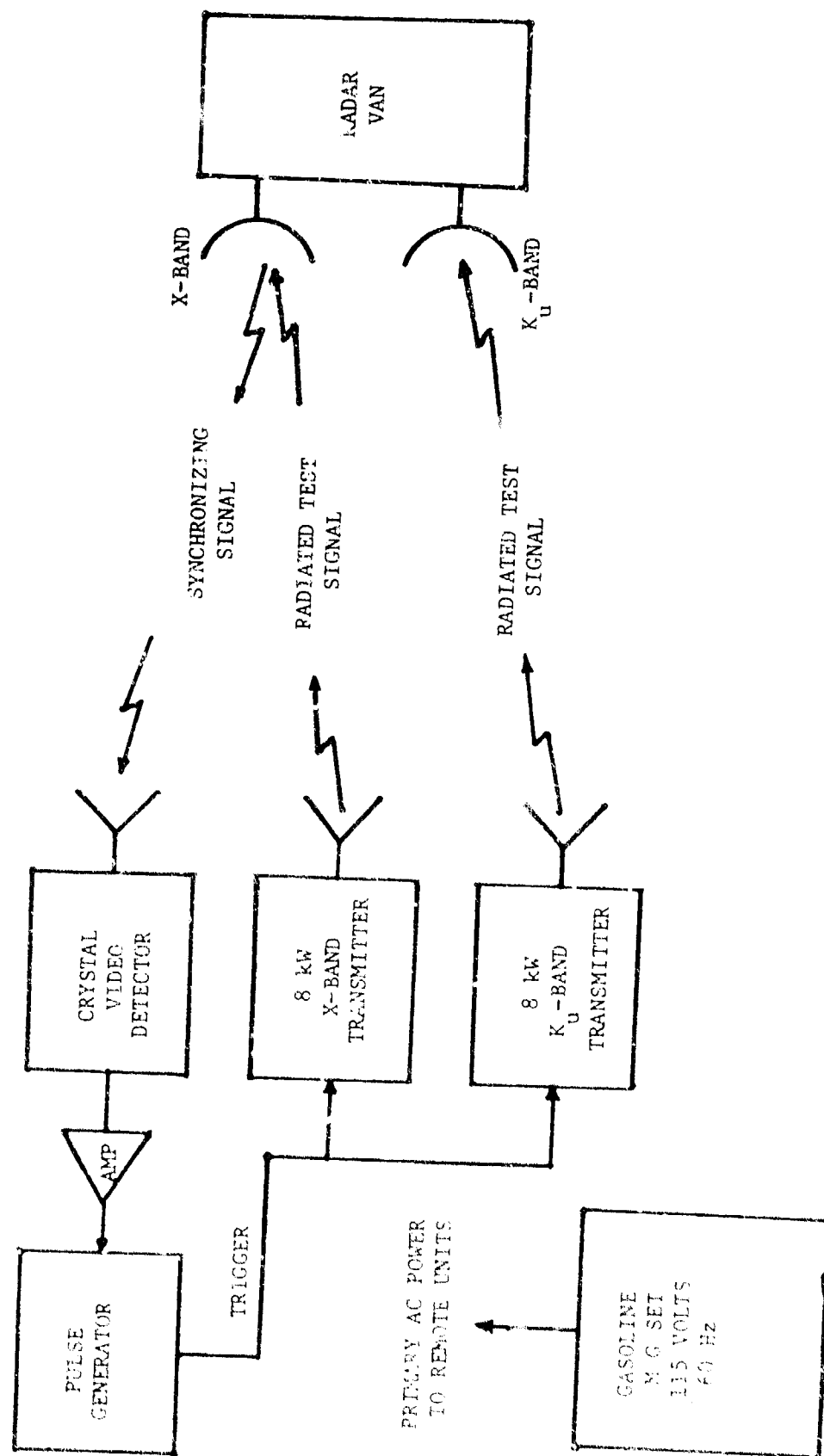
Figure 9. Block diagram of equipment configuration used in one-way measurements.
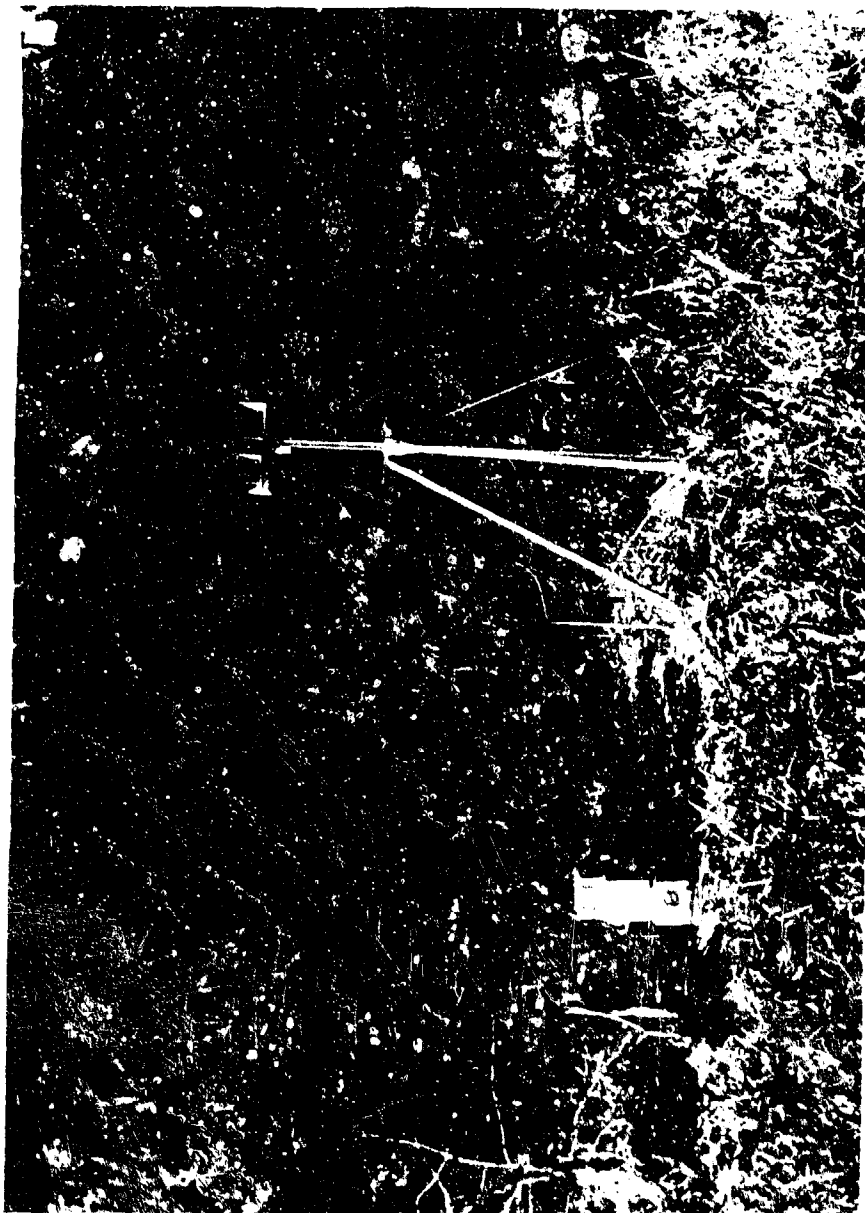
Figure 10. Remote transmitters and transmitting horns used in one-way experiments.
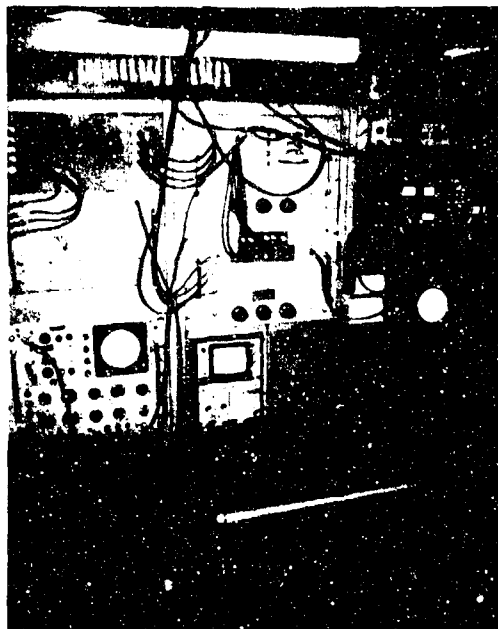
Figure 11. View of the operating console inside the radar van showing the "A and B-scope" displays and the data acquisition instrumentation.
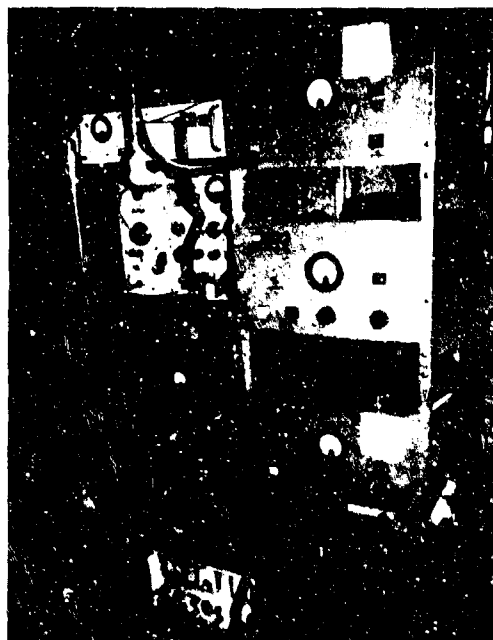
Figure 12. Close-up of the radar transmitter controls and the rf calibration equipment.

installed in the waveguide between the antenna and the receiver mixers. The receiver calibration or transfer function is generated by attenuating the injected signal level in 10 dB increments from 0 dBm through the receiver noise level and recording the sampled video on magnetic tape. Signal losses between the receiver inputs and the directional coupler are added to the calibration levels in the data-reduction program in order to determine the received power level at the receivers.

A signal generator is not available to calibrate the 95 GHz radar. Calibration of this system is achieved by placing a corner reflector of accurately known radar cross-section in front of the radar. A receiver transfer function is generated by varying an rf attenuator in 10 dB steps as was done for the other radars. Calibrations achieved in this manner are directly related to the radar cross-section of the reference corner reflector and yield accurate results if site-dependent factors are taken into consideration.

3. Measurement Procedures

The collection of radar data requires that careful attention be directed towards developing a set of procedures and definitions which will adequately present a proper framework for interpretation. Although the primary concern here is for the attenuation factor, which is a relative quantity, full calibration procedures were followed so that the data obtained here can be analyzed for backscatter coefficients, etc. if desired. The detailed step by step procedure for check-out and calibration of the radars and associated instrumentation is included in Appendix A. This procedure is routinely followed and ensures a high degree of confidence in the numerical value of the raw data. However, specific problems associated with foliage definition, near-field effects, and multipath effects had to be addressed before a fully satisfactory procedure could be developed which would lead to confidence that the data are truly representive of the actual foliage attenuation.

Preliminary experiments were conducted at the field site to determine a satisfactory criterion by which foliage depth could be measured. Several experiments were conducted in which a corner reflector or a signal source was placed in a clear area and then moved back into a foliated area. The

21

differences between the signal levels received at the radar for the two conditions were calculated. This difference represents the total attenuation of the signal due to the added foliage and when divided by the path length is the attenuation coefficient with units of dB/unit length. After several experiments at various depths into the foliage, it was determined that the measure of foliage depth which led to the least variability in the attenuation coefficient was a summation of the actual measured depth of each individual tree branch in the signal path. This criterion not only led to the least variability in the data, but also led to good agreement between the one-way and two-way measurements.

The effects of multipath had to be considered before measurements were made, since the corner reflector or sources had to be moved during these experiments. Radiated waves propagating over different paths and arriving at the same point vectorially sum to create nulls and lobes in the energy field. To determine if ground reflections were a problem, a field probe was placed at the clear measurement location. Figure 13 illustrates the effect of ground reflections at the measurement site. The field probe was a 4-meter- high aluminum pole with a corner reflector attached to a motor-driven mount which was uniformly raised in height above the ground while the return power at the radars was measured. The measured power at the radars was found to be constant above a height of 3 meters at the four measurement frequencies.

Near-field effects were noticed when intervening foliage was near the corner reflector or horn antennas. These effects were verified experimentally by placing cut branches at various distances in front of the corners and horns and measuring the received power. Large variations in received power were present when the foliage was located within one meter of the corner or horns. At a distance of 3 meters, power variations were sufficiently small so as to be attributed to movement within the foliage rather than disturbances within the near-field region of the horns. The near-field distance based on the horn dimensions is approximately 2.5 meters. The dimensions of the corner reflectors (up to 55 cm) used in the experiments were so large that a far-field criterion could not be met in all cases, because of the natural environment in which the experiments were conducted. Meeting the far-field criterion is perhaps academic for these measurements, since, among other things, the foliage itself may be considered a new source of radiation
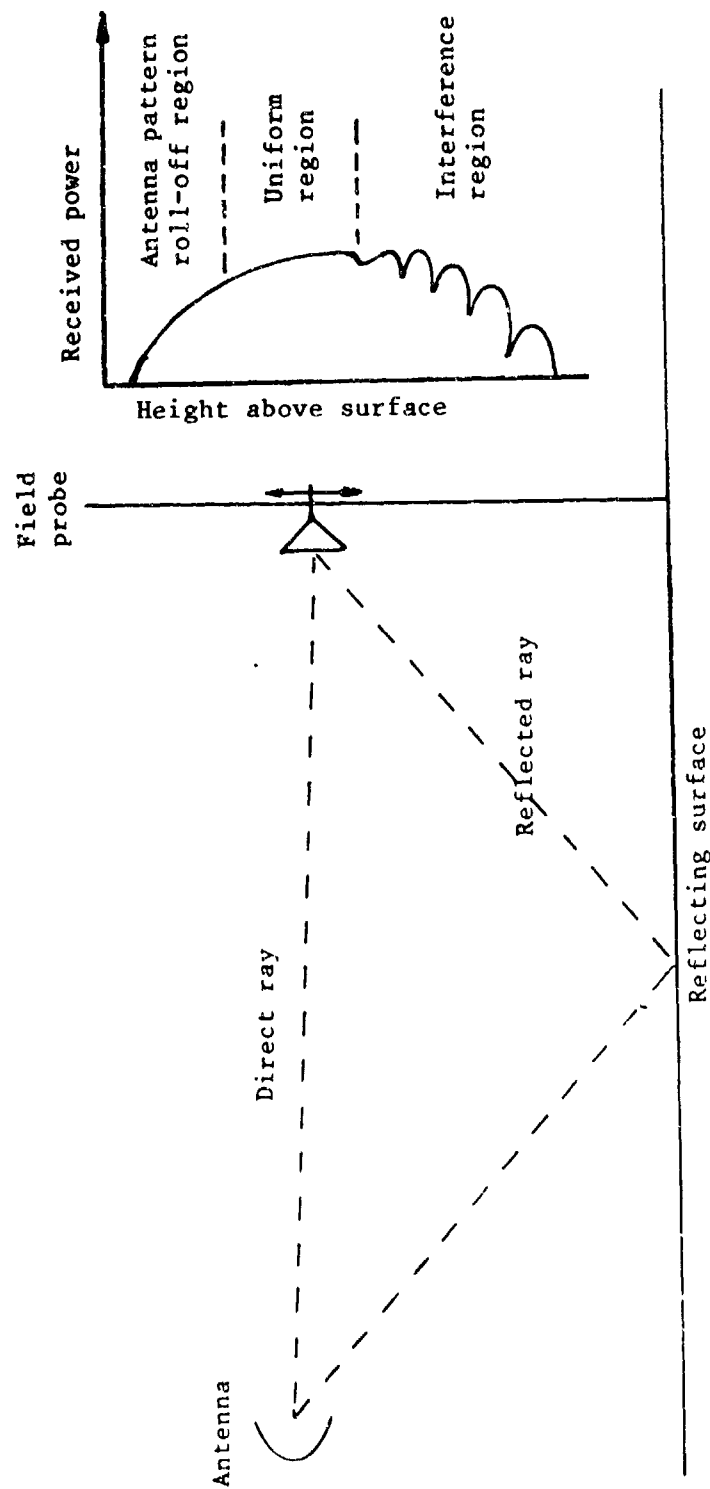
Figure 13. Illustration of the effect of ground reflections on the field pattern of the radar. The maximum height of the interference region was 3 meters above the surface.

23

with extremely large dimensions, resulting in a nonuniform phase front out
to great distances.   In addition, targets, such as vehicles, located under
a tree canopy will normally have sufficiently large dimensions that the near
field of the reflected wave will extend beyond the canopy.   In these experi-
ments, however, the far-field criterion was generally satisfied for the
one-way measurements, and as much distance as possible was allowed between
the foliage and the corner reflector for the two-way measurements.

Based on the results of these preliminary experiments, a set of procedures
to be followed in setting up the remotely located equipment was established.
A detailed list of these procedures is included in Appendix B.   In setting
up the remote equipment, all locations in the foliage were marked on a radial
path between the clear reference point and the radar van.   In the two-way
experiments, measurements were made at three lateral locations spaced approxi-
mately 1/3 meter apart at each foliage depth.   In the one-way experiments,
measurements were made at the three lateral locations and also at heights
of 3, 3.4, and 3.8 meters.   This procedure allowed either three or nine
samples over the same general foliage path for the one-way and two-way
experiments, respectively.   Video samples of the signals were recorded for
one minute at each location.

II. DATA ANALYSIS

A. Data Analysis Techniques

The data obtained from the radar penetration measurements consisted primarily of fm magnetic tape recordings of amplitude fluctuations of the received signals from the remote transmitters or corner reflectors for the one-way and two-way experiments, respectively. Strip chart recordings, A-scope photographs, and other miscellaneous data such as log sheets of wind-speed and direction, provided background information to supplement the magnetic tapes, but were not analyzed directly.

1. Data-Reduction Facility

Data-reduction facilities of the Advanced Sensors Division and Radar Technology Division of EES were used to process the magnetic tapes from the radar foliage penetration tests. Figure 14 gives a view of the typical data facility components. These include the following: (1) An analog signal-conditioner unit which provides variable gain and offset to allow the interface of varied types of signals to the data-reduction facility. (2) A Fabri-Tek Model 1072 Instrument Computer which serves as an A/D and D/A interface, and also computes real-time pulse-height distributions. The D/A output from the Fabri-Tek computer can be displayed on a CRT display or can be plotted on an x-y plotter. In addition, an Ubiquitous Model VC-202C Computer was also used to calculate distributions in parallel with the Fabri-Tek.; (3) A PDP-8/F computer which can exchange information directly with the Fabri-Tek computer; (4) A teletype; (5) A Digital Equipment Corporation Decassette Recorder for program development and storage.

The PDP-8/F computer contains 16K of memory, of which 8K is magnetic core. An extended version of FOCAL$_{TM}$ has been developed for use with the PDP-8/F and is designated FOCL/F. [4] This language is interactive and greatly facilitates program correction and modification. Also available is an in-house developed machine language software package for calculating fast Fourier transforms (FFT), and a set of software commands for Fabri-Tek control. These two machine language software packages along with the
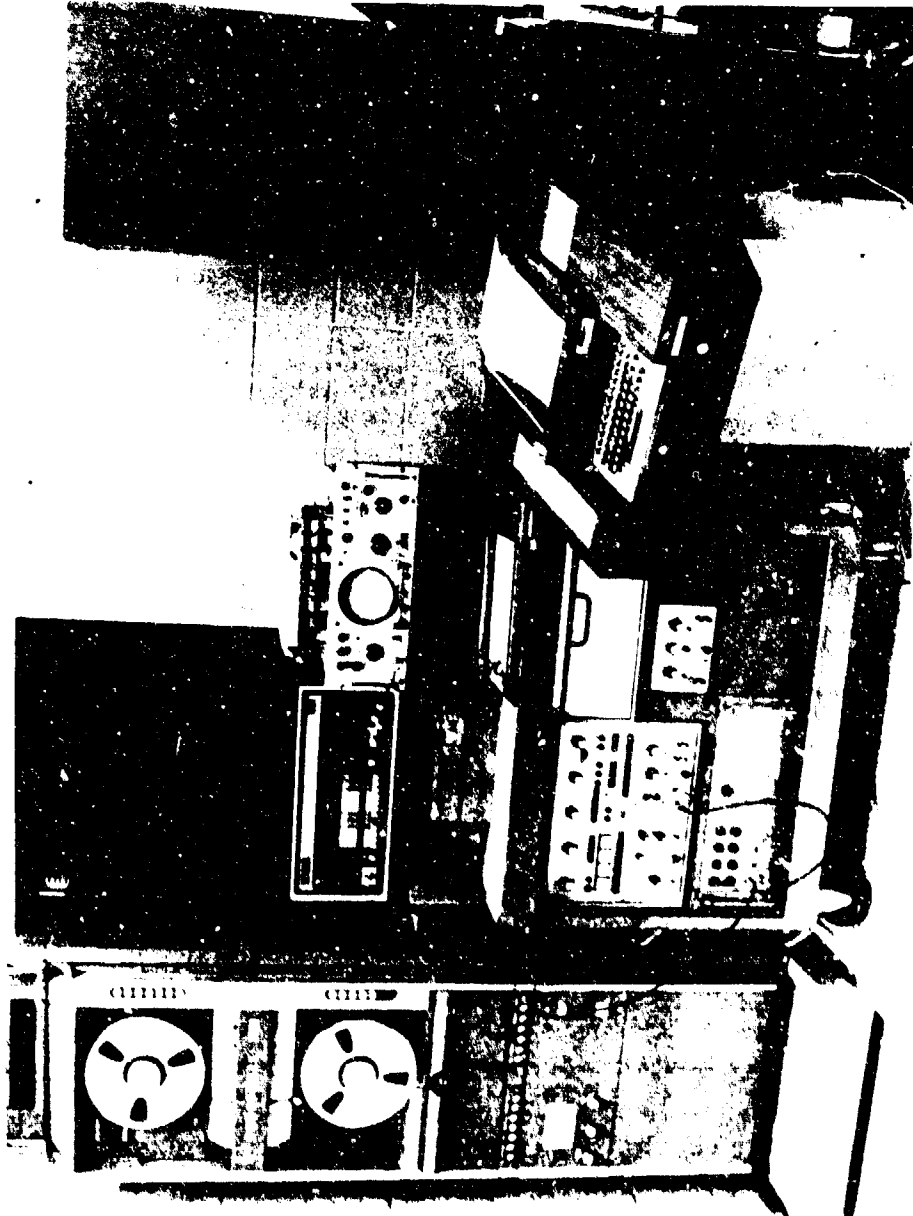
Figure 14. View of the PDP-8/F based data reduction facility.

extended FOCAL$_{TM}$ software make this system a very powerful and flexible data-reduction facility.

2. Data Analysis Procedure

The types of analyses which are normally obtained from the data facility include: (1) pulse-height amplitude (PHA) distributions, (2) frequency spectra, and (3) auto- and cross-covariance functions. The methods for obtaining these three classes of results are sufficiently different as to require entirely different FOCAL$_{TM}$ programs for their calculation. Results from these three types of analysis have been used to characterize the recorded data.

a. Pulse-Height Amplitude Distributions

Pulse-height amplitude distributions calculated by the data facility are displayed in two forms: as probability density plots and as probability distribution functions. The probability density plots are generated from data time histories from the magnetic records. The analyzer samples the input analog time history, A/D converts the samples, determines into which of 1024 amplitude bins the sample belongs, and increments a stored variable corresponding to the number of samples which have fallen in that amplitude window. When repeated a large number of times, this process generates a voltage amplitude distribution which is then calibrated and divided by the total number of samples to achieve a normalized probability density function. Approximately 30 seconds of data were used to generate the distributions analyzed resulting in about 60,000 samples. Assuming a decorrelation time of 50 milliseconds at X-Band, this results in about 6000 independent samples for the worst case.

The voltage amplitude distributions are calibrated by reference to a known comb (amplitude) signal. The peak of the distribution for each voltage step in the calibration comb is assigned the dB value corresponding to that calibration step. The PHA program in the PDP-8/F then does a cubic fit to the calibration and generates an equation relating dB value and amplitude bin number. The cubic fit program was developed to "linearize" nonuniform calibration steps so that the output density functions can be plotted on a linear scale.

The probability distributions are calculated by point-by-point numerical integration of the probability density functions. The functional values of these distributions are then multiplied by a nonlinear transfer function so that they can be plotted on probability paper.

The resultant probability distributions are useful in determining the median values of the distributions and also their shapes. In addition, for certain classes of functions, the average values can be determined from the distributions using a simple formula.

b. Frequency Spectra

The frequency spectra data-reduction program uses the fast Fourier transform subroutines available for the PDP-8/F to transform input time histories to the frequency domain. The program has several options which allow the spectral data to be presented in different forms including: (1) voltage amplitude versus frequency, (2) normalized log voltage amplitude in dB versus frequency, (3) normalized linear voltage amplitude in dB versus frequency.

The voltage amplitude program in the PDP-8/F computer processes an input time history which has been sampled, A/D converted, and stored by the Fabri-Tek. The program computes the fast Fourier transform for that time history, and calculates the square root of the sum of the squares of the real and imaginary parts of each element in the transform. Since a time history typically represents the voltage out of a logarithmic receiver, which is proportional to the logarithm of the received power, the amplitude of the spectrum corresponding to the time history is measured in dB relative to a milliwatt (dBm). Thus, to calibrate the spectral amplitude in dB, a calibration is stored in memory which relates dB values to input voltage amplitudes, and each time history is converted to dB values as it is read in. Since the Fourier transform is a linear process, the spectrum amplitude will be proportional to dB if the time history is calibrated in dBm and the proportionality constant is set equal to one in the program.

Figures 15 and 16 give typical time histories for 9.4 GHz and 95 GHz. The vertical scales represent received power in units of dB. A time history is limited in duration to the number of Fabri-Tek memory bits times the sample period. For this case, the sample rate equals the prf used in taking the data (2000 Hz), so that a time history is given by: 1/2000 x 1024 = 0.512 seconds. To achieve the equivalent of a longer time history, the Fourier transforms of eight adjacent time histories are averaged together.
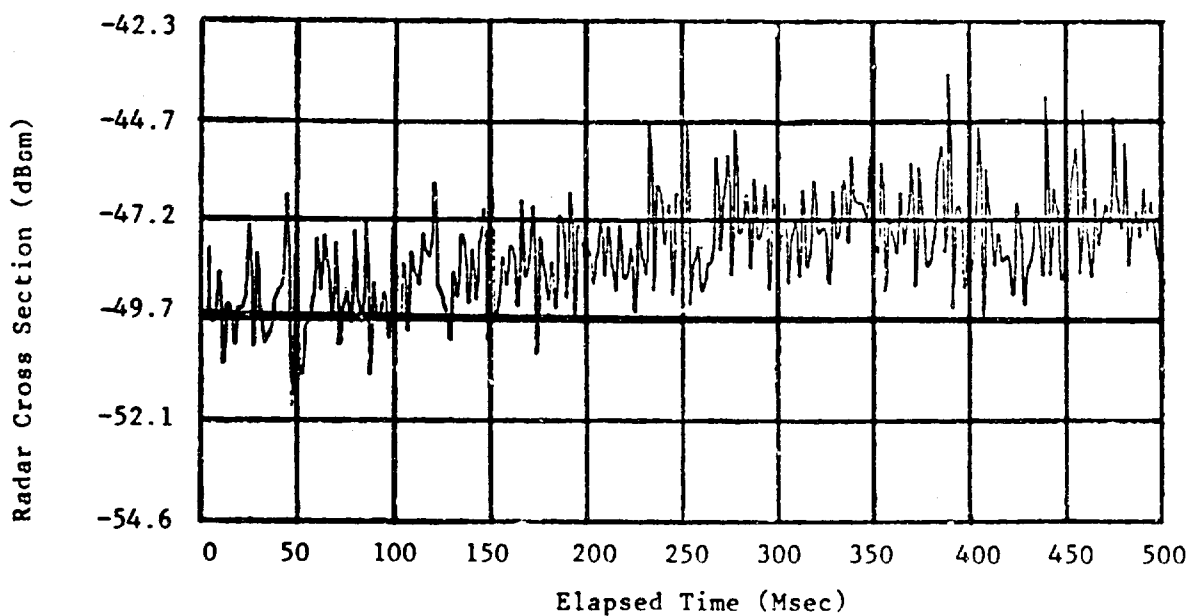
Figure 15. Time history of the recorded return from a corner reflector immersed in foliage; 9.4 GHz, vertical polarization.
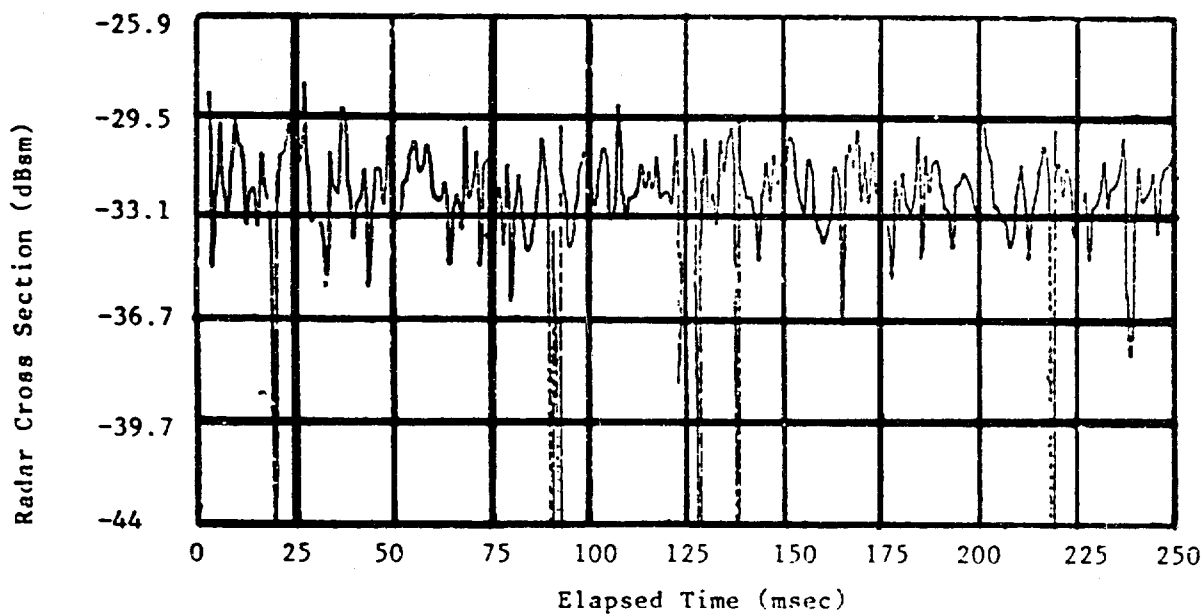
Figure 16. Time history of the recorded return from a corner reflector immersed in foliage; 95 GHz, vertical polarization.

29

The actual number of time histories averaged is arbitrary; however, previous experience has shown that eight to ten are sufficient to establish a reasonable short-term average.

In calculating the FFT, the dc term has been set to zero because its amplitude is normally so much larger than the rest of the spectrum that dynamic range problems are encountered in the computer due to the form of the FFT algorithm. Thus, the zero frequency point is zeroed in all the plots. However, this dc point can still be determined independently from the amplitude distribution functions.

A second method of displaying the log amplitude spectrum is to normalize the spectrum by dividing all the elements by the peak element value. The spectrum is then plotted in dB relative to the peak voltage amplitude, which is normally the lowest frequency point. This type of plot is very useful for comparing frequency roll-off characteristics of spectral plots with different amplitudes.

Although the data recorded on the magnetic tapes represent the voltage output from a logarithmic receiver, it was deemed desirable to plot the equivalent spectrum for a linear receiver. Therefore a modification was developed to the spectrum program which allowed the "delogging" of the input data prior to calculation of the Fourier transform. When normalized, this program results in the calculation of the normalized linear frequency spectrum. For certain classes of functions, to which all the data processed here belong, this power spectrum is equivalent to the power spectral density. The unnormalized calibrated power spectrum cannot be determined by this method since the dc term is thrown away, as previously described.

c. Auto- and Cross-Covariance Functions

The auto-covariance functions and cross-covariance functions for input time histories are determined by similar methods in the data analysis. Auto-covariance functions are computed from the inverse transform of the magnitude of the Fourier transform squared in the PDP-8/F computer, while cross-covariance functions are computed from the inverse transform of the product of the Fourier transforms of two time histories which are sampled

30

simultaneously.

The normalized cross-covariance function is thus given by

$$C_{xy}(\tau) = \frac{F^{-1}[F_x(j\omega) \cdot F_y^*(j\omega)]}{\sqrt{C_{xx}^2(0) \cdot C_{yy}^2(0)}}$$

where F_x and F_y are the Fourier transforms of the respective functions $f_x(t)$ and $f_y(t)$ with the dc terms set to zero and C_{xx} and C_{yy} are the respective auto-covariance functions for f_x and f_y.

Due to the limited memory length available in the Fabri-Tek, the total delay time available using the stated method for computing correlation functions is given by:

$$\tau \ (\text{seconds}) = \frac{1024 \ \text{memory words}}{2000 \ \text{samples per second}} = 0.512 \ \text{seconds}$$

This delay time can be increased by lowering the sample rate at the cost of resolution. (A 0.5 millisecond resolution is achieved for a 2000 Hz sample rate.)

B. Summary of Results

1. Interpretation of the Data

The propagation data presented in this report were obtained for the most part at grazing angles below 3°. The reasons for this limitation in the experiment were of a practical nature, since the two-way experiment could not be performed for high depression angles because of the large attenuations encountered when trying to penetrate a moderate size tree canopy. Therefore, the two-way experiment was performed on the foliage at the edge of a tree line allowing the foliage attenuation characteristics to be probed as a function of depth. The one-way experiment was performed over the same geometry so that the one-way and two-way results could be directly compared. In addition, a high depression angle experiment (29°) was performed for the one-way case so as to tie the low angle results to the high angle case of interest. Because of the lack of equipment at 35 GHz and 95 GHz, the one-way experiments could be performed at 9.4 GHz and 16.2 GHz only, while the two-way experiments were performed at all four frequencies.

31

One of the most serious difficulties encountered during the test program was the problem of developing a suitable definition of foliage depth. As is obvious from examining a tree, its foliage canopy is not uniform, being grouped into branches often with large open areas between the branches. Also, the outside layers of foliage of a tree tend to be more thickly foliated because of the absence of sunlight in the interior parts of the tree. In addition, within a given branch, the location of the foliage and limbs can be very nonuniform, and most certainly the uniformity varies with tree type.

After some experimentation, it was determined that a foliage definition based on layers of foliage in the path of the radar beam works fairly well. For this definition, the foliage thickness is computed by determining the number of branches or foliage layers in the beam path, measuring the gross thickness of each layer, and summing the depths of the various layers to obtain the total thickness. The nonuniformity of the layer densities are ignored because of the difficulties in determining these densities. Obviously, since individual branches on a tree and also different trees do have different foliage densities, there are some errors in the foliage depth estimates using this method. However, it was determined that the spread in the foliage attenuation coefficients measured caused by the inability to characterize the foliage densities exactly was less than a factor of two-to-one for a very densely foliated branch as opposed to a very light one. It was also noticed that differences in the attenuation coefficient measured for individual branches on a given tree were greater than the average differences between types of trees including deciduous and coniferous trees.

An alternative definition for foliage depth which makes some sense in terms of the relative ease of depth estimation, is the total line-of-sight distance through the tree canopy along the beam path. Use of this definition results in much lower values of the attenuation constant, since typically more than 50% of a path through a tree canopy is open space. The average total attenuation through a given tree canopy should be the same regardless of which definition of attenuation constant is adopted; however, the variation of the values measured for attenuation coefficient for a given tree group will increase if the total-path-length definition is used, because the actual

foliage in the beam path changes for different parts of the tree, thus causing the measured attenuation to change while the line-of-sight path length does not change.

Previous measurements of foliage attenuation have been concentrated in the frequency region 50 to 3,000 MHz, with the primary emphasis on propagation of one-way television and communications transmissions. Also, many of the experiments have been performed with CW equipment so that their applicability to the high-frequency pulsed-radar case is in doubt. Moreover foliage depth has been determined by measuring the line-of-sight distance through a forest, ignoring spaces between trees and spaces between the tree limbs, a procedure which results in obvious problems in obtaining consistent values of the attenuation constant.

However the results of some of these low-frequency experiments can be used to estimate "ball park" values for attenuation for the higher frequency pulsed radar case. Nathanson has derived an equation for attenuation coefficient as a function of frequency for data between 100 to 3,000 MHz compiled by Saxton and Lane which is given by: [6] [7]

$$A(dB/m) = 0.25 \ f^{3/4} \qquad (3)$$

where f is in GHz.

This would yield values for the attenuation coefficient of 0.25 dB/m at 1 GHz, 1.4 dB/m at 10 GHz, and 7.9 dB/m at 100 GHz. The foliage depth estimates for these measurements were based on the line-of-sight distances through a forest, and thus result in lower values for the attenuation coefficient than the definition used for the present penetration measurements (foliage layers). However, Nathanson's equation can be compared with the new data obtained under the present program as a check of the consistency of the new data. The attenuation coefficients calculated using the two different definitions of foliage depth can be approximately related if it is assumed that a given forest is approximately 50% foliage and 50% open space. Thus, the equivalent attenuation values given by Nathanson's equation would be approximately half as great as the attenuation constants determined using the foliage layer definition.

33

2. Penetration Data Summary

As was discussed in a previous section, penetration data were obtained at three sites during the tests. Both one-way and two-way data were obtained at Sites 1 and 2, while only one-way data were obtained at Site 3, which allowed much higher depression angles than Sites 1 and 2. The following sections will discuss the properties of the data obtained at all three sites.

a. Attenuation Coefficient

Figure 17 gives the distribution of the attenuation coefficient data in dB/m obtained for the one-way measurements at 9.4 GHz and 16.2 GHz at Sites 1 and 2, including both horizontal and vertical polarizations, and Table 6 gives a summary of the oneway data as a function of frequency and polarization. Table 6 shows that the median values obtained for the attenuation coefficient were slightly lower than the mean values, and differences in the median values for vertical as opposed to horizontal polarization were small; much less than one standard deviation. The data represented by the summary consisted of about 50 individual data runs, each run consisting of about 30 seconds of data at a given depth in the foliage. The data summary includes both deciduous and pine trees, since the differences in the attenuation coefficients between types of trees were less than the variations within a given tree type due to different foliage densities.

Figures 18 and 19 give the distributions of the two-way data at 9.4, 16.2, 35, and 95 GHz, while Table 7 summarizes the results as a function of frequency and polarization for dry foliage at Sites 1 and 2. The data at 9.4, 16.2, and 35 GHz represent about 50 data runs as in the case of the one-way data, while the data at 95 GHz represent about 25 runs because of some equipment problems in the field.

As in the one-way case, the median values of the attenuation coefficient are less than tne mean values and there is little difference between the results for vertical polarization and horizontal polarization although the horizontal values are slightly higher. The median values of attenuation coefficient do increase with transmitted frequency, being proportional to the logarithm of the frequency. Also the standard deviations of the mean values of the data increase with frequency, indicating the measured values of attenuation vary more widely with increasing frequency. This is not unexpected

34
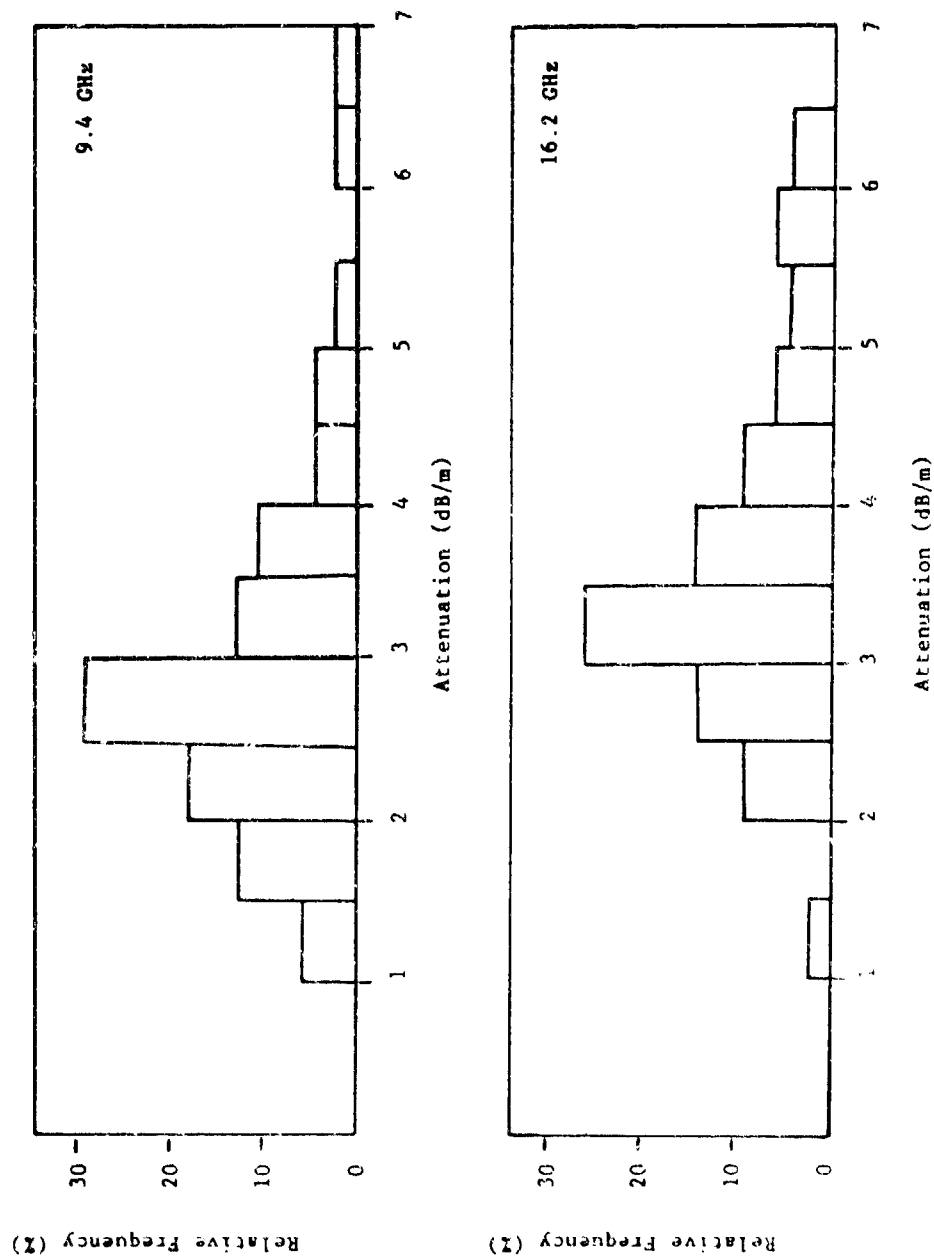
Figure 17. Relative frequency of occurrence of the attenuation coefficient for one-way penetration measurements; 9.4 GHz and 16.2 GHz.

TABLE 6

SUMMARY OF ONE-WAY ATTENUATION MEASUREMENTS

Frequency	9.4 GHz		16.2 GHz	
Polarization	V	H	V	H
Median	2.6	2.7	3.7	3.3
(dB/m)				
Mean	2.7	3.1	3.8	3.5
(dB/m)				
Std. Deviation (dB)	0.7	1.4	1.2	1.1
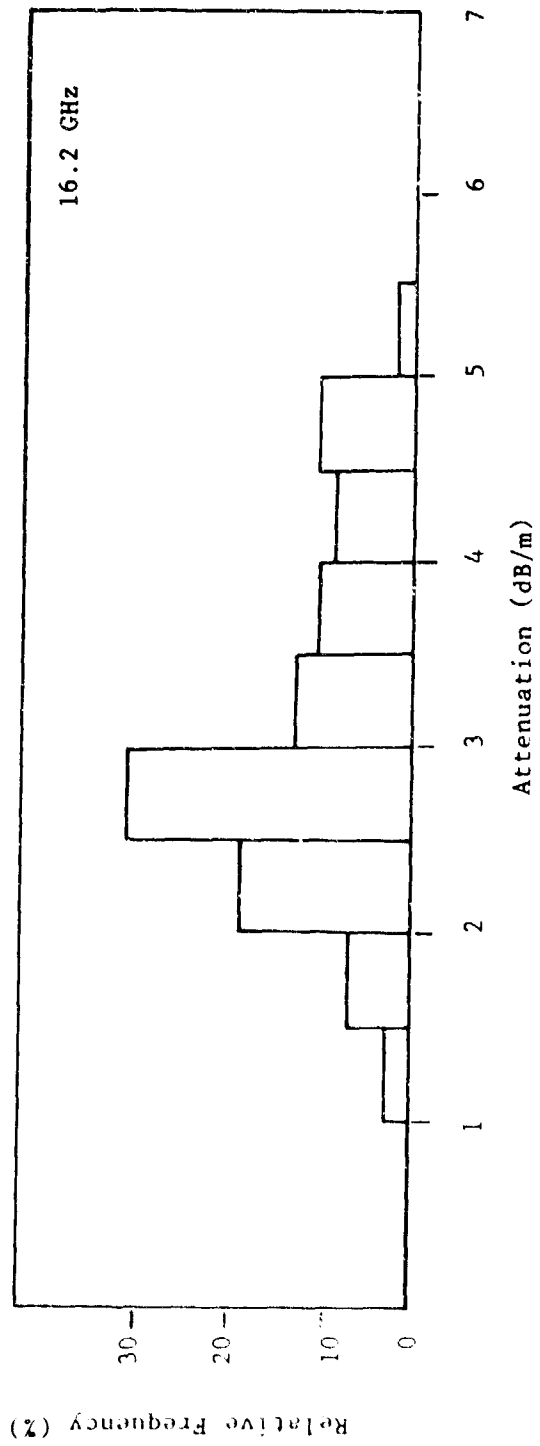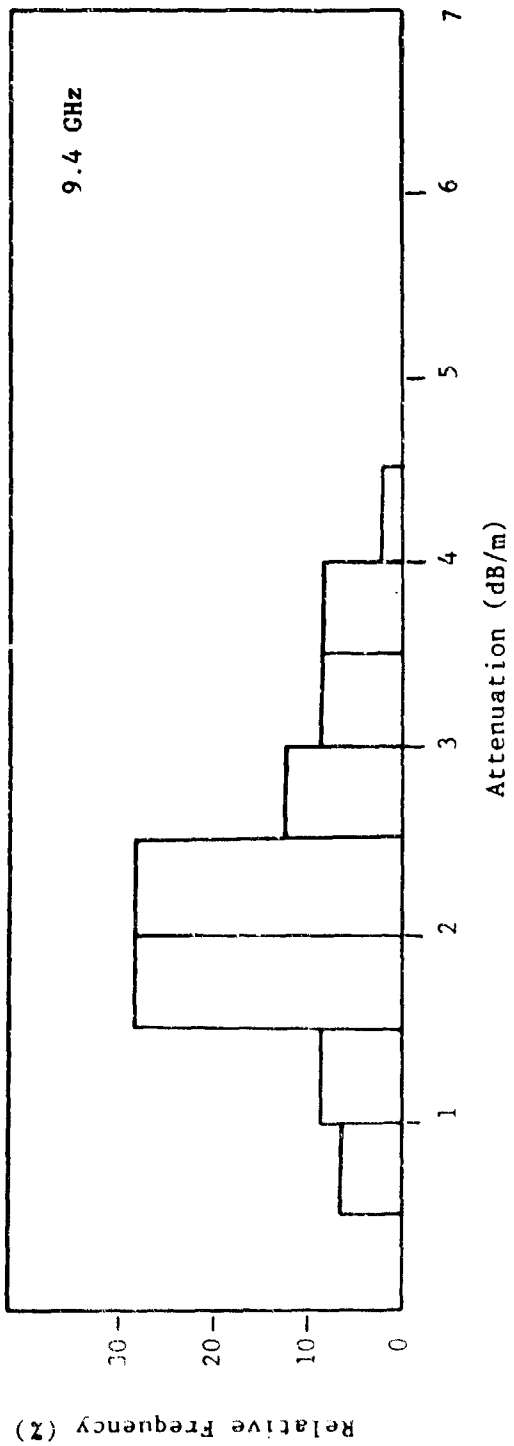
Figure 18. Relative frequency of occurrence of the attenuation coefficient for two-way penetration measurements; 9.4 GHz and 16.2 GHz.
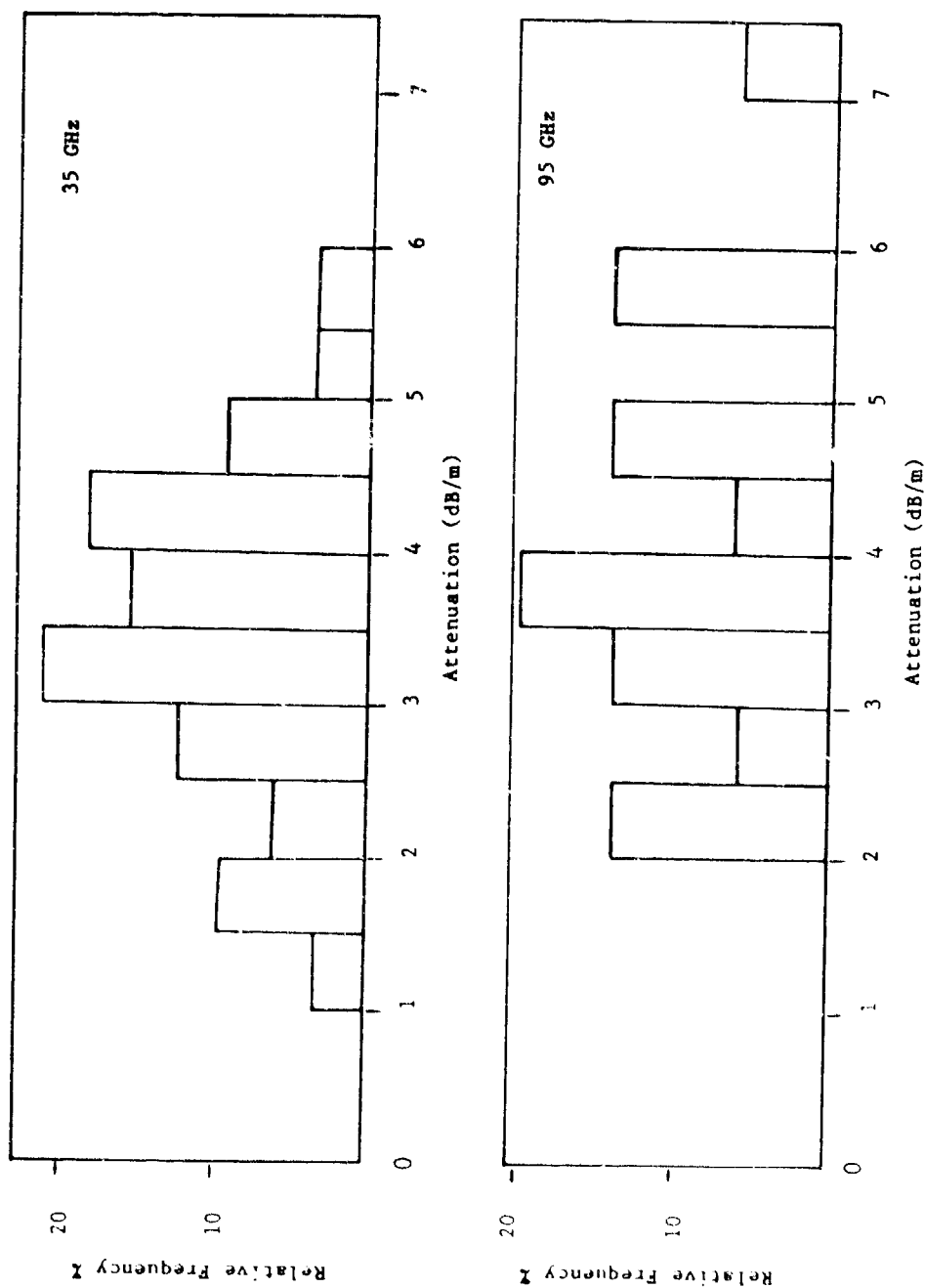
Figure 19. Relative frequency of occurrence of the attenuation coefficient for two-way penetration measurements 35 GHz and 95 GHz.

TABLE 7

SUMMARY OF TWO-WAY ATTENUATION MEASUREMENTS

Frequency	9.4 GHz		16.2 GHz		35 GHz		95 GHz
Polarization	V	H	V	H	V	H	V
Median (dB/m)	1.9	2.3	2.7	3.1	3.4	3.3	3.9
Mean (dB/m)	2.0	2.5	2.7	3.5	3.7	3.0	4.1
Std. Deviation (dB)	0.84	0.61	0.76	1.10	0.30	1.56	1.30

39

since a wavelength is less than the size of the individual twigs and leaves at the higher frequencies.

There is a slight difference between the median values for attenuation coefficient for the one-way and two-way cases of about 0.5 dB. This is assumed to be due to the differences in the illumination functions between the standard-gain horns used in the one-way measurements and the corner reflectors used for the two-way measurements, and also due to the fact that a number of one-way measurements were made at larger depths than the two-way measurements. It was discovered during the tests that the attenuation coefficient varies as a function of foliage depth. Since the foliage depth at which a measurement can be made is limited by the backscatter from the foliage for the two-way case and also since the attenuation is twice as great as for the one-way case, the foliage depth for which a two-way measurement can be made is much less than for the one-way case.

However, since the differences between the one-way and two-way data were small, all the data at 9.4 GHz and 16.2 Ghz were grouped together, and the resulting distributions are given in Figure 20. The median values of these combined distributions, 2.5 dB/m at 9.4 GHz and 3.1 dB/m at 16.2 GHz, will be used as the attenuation coefficient values at 9.4 and 16.2 GHz presented later in this report.

Table 8 summarizes the one-way high-depression-angle measurements that were made at Site 3. The geometry of this site was a more realistic simulation of the mini-RPV situation, since the depression angle was 29°, and the average foliage depth (using the foliage layer definition) was greater than 5 meters. The tree for which the measurements were performed was a densely foliated water oak. The measured median values of attenuation coefficient were 3.2 dB/m at 9.4 GHz and 4.2 dB/m at 16.2 GHz. These values are higher than the median values of the data obtained at Sites 1 and 2 for small depression angles. This is probably due to the fact that blockage due to large limbs was more prevalent for the high depression angle, since the trees at Sites 1 and 2 were smaller than the large tree utilized for the high-angle experiment.

It should be noted that the average line-of-sight path length through the tree was almost three times the mean foliage depth so that if the attenuation coefficient is calculated using the path-length definition of the foliage, the values are much lower and in fact come very close to fitting Nathanson's equation. (See Equation 3.)
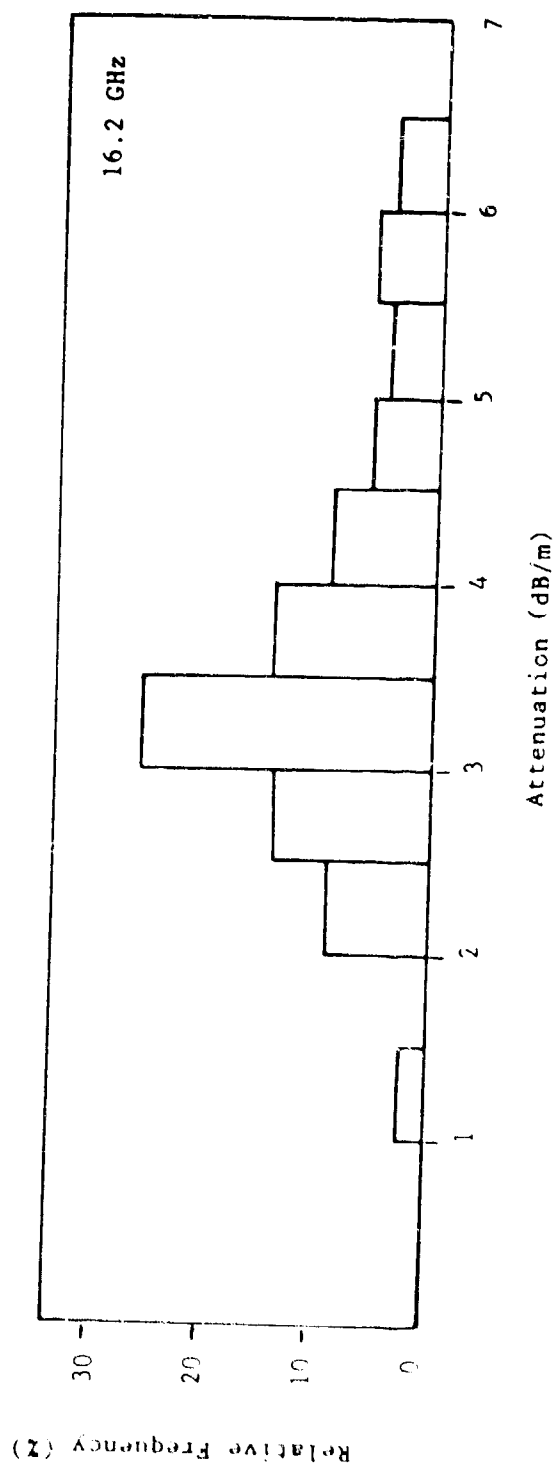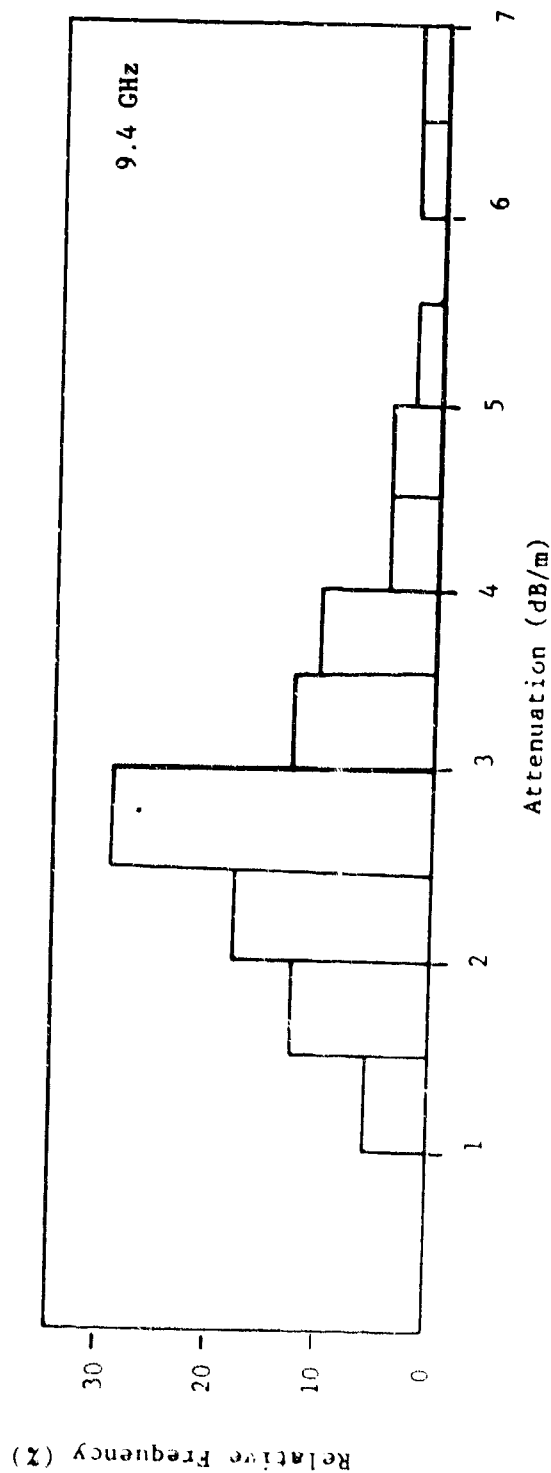
Figure 20. Relative frequency of occurrence of the attenuation coefficient for the combined one-way and two-way penetration measurements; 9.4 GHz and 16.2 GHz.

TABLE 8

Large Depression Angle Measurements

Frequency	9.4 GHz	16.2 GHz
Median Attenuation (dB/m)	3.2	4.2
Mean Attenuation (dB/m)	3.4	4.2
Std. Deviation (dB)	0.38	0.40
Mean Attenuation Over Path (dB)	19.8	22.4
Mean Path Length (m)	15.6	15.6
Mean Foliage Depth (m)	5.8	5.4
Loss Per Meter Based on Mean Path Length (dB/m)	1.29	1.44
Loss Per Meter Based on Mean Foliage Depth (dB/m)	3.4	4.2

b. Depth Dependence of Attenuation

For two foliage areas at Site 1 it was possible to conduct experiments to explore the attenuation dependence versus foliage depth.* For these areas, the foliage was approximately uniform for a distance of up to 10 meters into the foliage, so that the attenuation could be determined when the corner reflector (two-way experiment) was placed at 1 meter intervals within the foliage.

Figure 21 gives the results of this experiment at 9.4, 16.2, 35, and 95 GHz. It is obvious from the figure that the attenuation coefficient (slope of the curves) is not a constant but increases with increasing foliage depth. Also this deviation from a straight line becomes greater with increasing frequency. This may explain why the one-way measurements give higher values than the two-way measurements, since the one-way measurements were generally made for greater foliage depths.

The variation of the attenuation coefficient with depth is probably due to many factors, for example, direct penetration through holes in the foliage near the edge (particularly at the higher frequencies), and multiple scattering effects at the boundary of the foliage which sum with the direct signal received from the corner reflector. Clearly, more work needs to be done in order to determine what mechanism is causing this phenomenon. It is anticipated that the winter foliage measurements scheduled to follow the present program will provide some information on the effects of scattering since the trees will be defoliated and the bare limbs exposed.

The actual measured results for the attenuation coefficient are shown in Figure 22 for wet and dry conditions. In the Figure, the median values for all the attenuation coefficients measured for both horizontal and vertical polarizations are plotted versus frequency, and the standard deviations of the data are shown as vertical lines for the dry data. (There were not enough points for the wet data to establish standard deviations.)

A least-squares fit of a straight line to the dry values yields the following equation:

$$A(dB/m) = 1.102 + 1.48 \log_{10}F$$

---

*The foliage depth definition used for all of the Georgia Tech data is the foliage layer definition which yields higher average values for attenuation than the line-of-sight distance definition used by other authors.
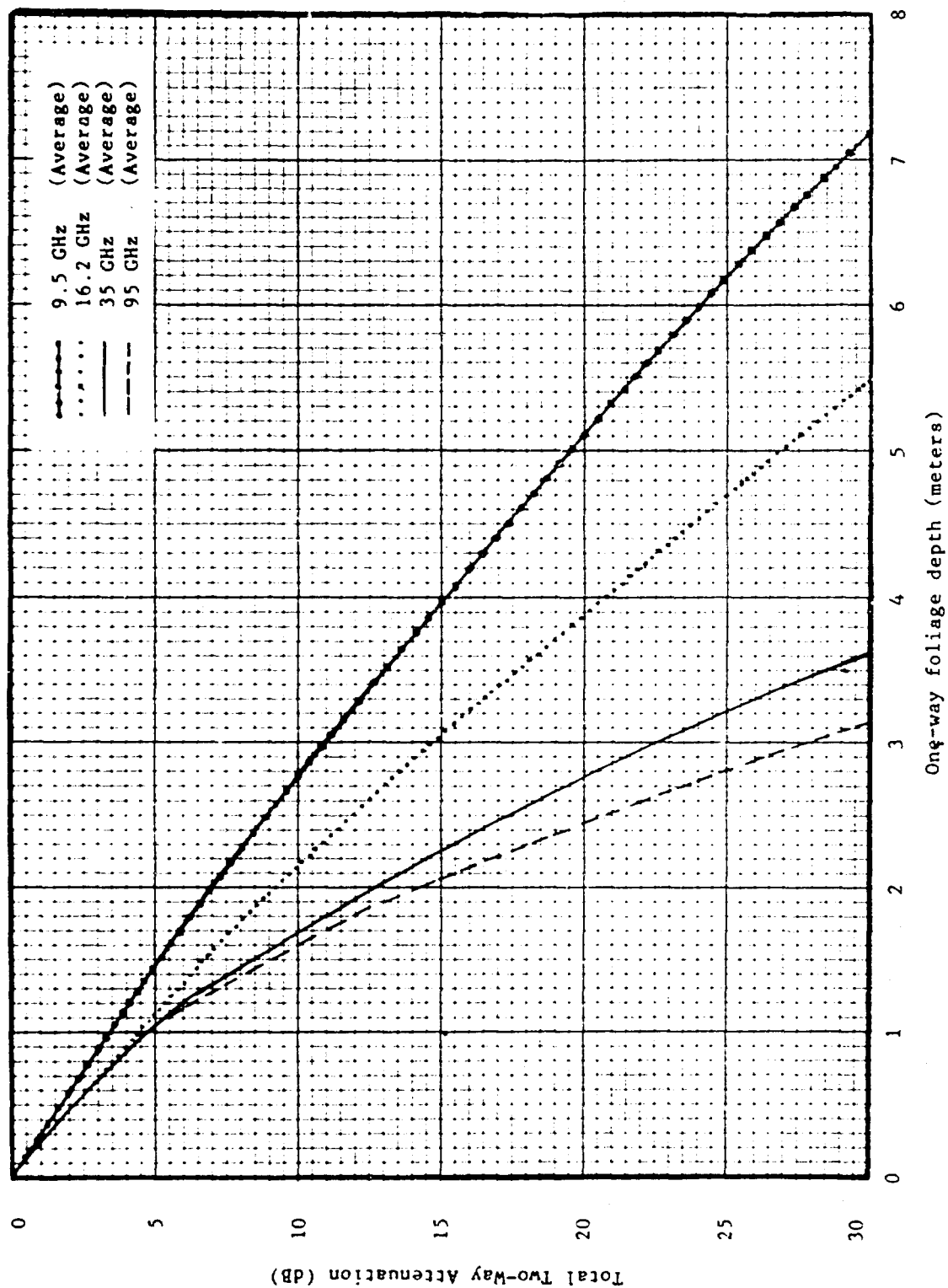
43

Figure 21. Total attenuation as a function of one-way foliage depth as determined by the two-way experiment.
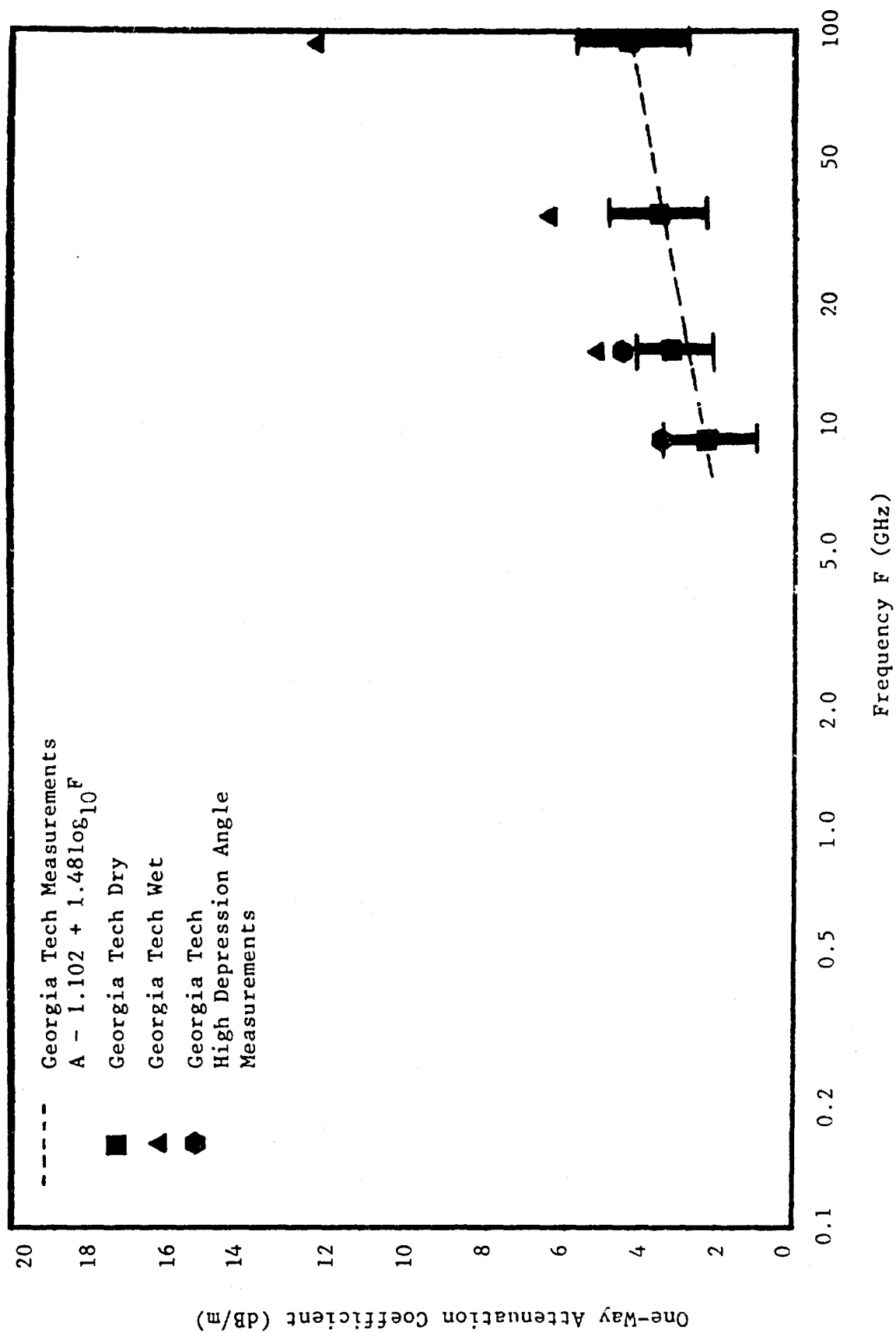
Figure 22. Median values of the measured attenuation constant data as a function of frequency for wet and dry conditions.

where F is in GHz.

This equation fits the dry data obtained at Sites 1 and 2. A limited amount of wet data was obtained at Site 1 and the results are also plotted in Figure 22. The wet values are much higher than the dry data and follow a power law rather than a logarithmic relationship as does the dry data. The high-depression-angle data (Site 3) are also plotted in Figure 22 and approximately fall on the wet data results, being higher than the dry, low-depression-angle data.

The data illustrated in Figure 21 suggest that the attenuation values for high depression angles, where the foliage depth is 5 to 10 meters, would be much greater than those measured for the present experiment, in which typical foliage depths were less than three meters. In particular, if the slopes of the asymptotes of the curves in Figure 21 are calculated, they yield 2.9 dB/m at 9.4 GHz, 3.8 dB/m at 16.2 GHz, 8.0 dB/m at 35 GHz, and 15.0 dB/m at 95 GHz. These values are much greater than the measured values at 35 and 95 GHz, and are slightly greater at 9.4 and 16.2 GHz. This is illustrated in Figure 23. The slopes of the asymptotes from the curves in Figure 21 are plotted versus frequency and it can be seen that these points can be fitted by Nathanson's equation multiplied by a factor of two. However, if the differences in the definition of foliage depth between the data used to determine Nathanson's equation and the present data are taken into account, it is not unreasonable to relate the two definitions by a factor of two (assume 50% foliage and 50% open space). Thus the slopes of the intercepts appear to verify Nathanson's equation which becomes (using the GIT foliage depth definition):

$$A \ dB/m = 0.5F^{3/4}$$

where F is in GHz, and A is based on a foliage layer definition.

In summary, the dry, low angle attenuation coefficient data follow a logarithmic law as a function of frequency but the asymptote slopes of the attenuation curves (Figure 23) appear to follow a power law that is very close to Nathanson's equation, if differences in foliage definition are taken into account. It is suspected that the measured data are low because of the relatively small foliage depths for which the measurements were made. For larger foliage depths, the results might approach the values of the asymptote slopes as the edge effects become a small contribution to the total attenuation.
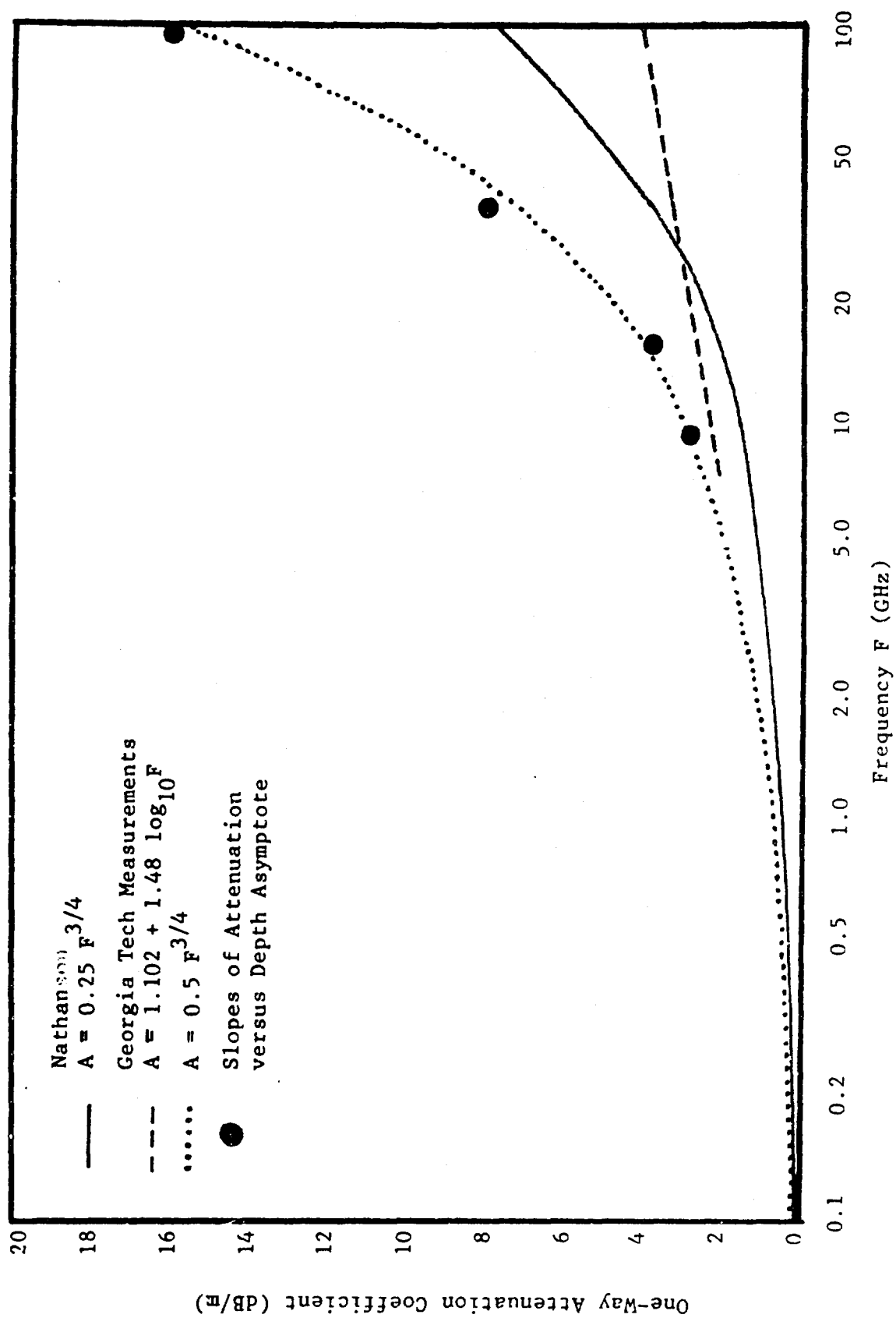
Figure 23. Comparison of the slopes of the asymptotes of the attenuation-versus-depth curves with the measured data.

The figure legend contains:

Nathanson
A = 0.25 F$^{3/4}$

Georgia Tech Measurements
A = 1.102 + 1.48 log$_{10}$F
A = 0.5 F$^{3/4}$

Slopes of Attenuation versus Depth Asymptote

Axes:
- Vertical axis (rotated): One-Way Attenuation Coefficient (dB/m), scale from 0 to 20
- Horizontal axis: Frequency F (GHz), scale from 0.1 to 100

c. Amplitude Statistics

Figures 24 through 27 give examples of the cumulative probability distributions of the received power frcm a corner reflector at 1 meter foliage depth intervals for 9.4 GHz, 16.2 GHz, 35 GHz, and 95 GHz. Each distribution represents 30 seconds of data or 60,000 samples at each depth. The left-most distributions represent the return from the corner at the edge of the foliage, while the distributions on the far right are due to the background reflections with the corner removed. Note the large change in power for runs between 1 meter and 2 meter foliage depths evident at 35 GHz and 95 GHz but not at the lower frequencies. This change possibly indicates that the first meter of foliage contained a number of holes which were penetrated at the higher frequencies, while the addition of a second meter of foliage filled in the holes, causing the attenuation to increase greatly.

The distributions are relatively narrow for the clear reflector runs and increase in width as the foliage depth increases. The 35 GHz and 95 GHz clear distributions are wider than the lower frequencies because the corner was buffeted by the wind, causing variations in cross-section which were more evident at the higher frequencies.

d. Polarization Properties

All the one-way and two-way measurements made at Sites 1 and 2 were dual-polarized measurements. That is, either vertical or horizontal polarization was transmitted, while both polarizations were simultaneously received. This allowed the polarization ratio of the received signal to be studied as a function of foliage depth. The orthogonal polarization characteristics were not analyzed in detail because of time and cost constraints but enough data runs were analyzed in order to obtain a general view of the depolarizing effects of intervening foliage.

Figure 28 gives comparative polarization results for one set of measurements at 35 GHz which is typical of the results obtained in general. In Figure 28 received powers for both the parallel channel (same polarization sense as the transmitted polarization) and the cross channel (orthogonal to transmitted polarization), normalized to the return from the parallel channel in the clear, are given as a function of foliage depth (left scale on graph). The parallel-to-cross ratio for the two received signals (right scale on graph) is also given as a function of the foliage depth. The power level of parallel channel decreases approximately linearly with depth for this run while the cross-channel level increases at 1 meter of depth over

48

Figure 24. Cumulative probability of the received power from a corner reflector as a function of foliage depth; 9.4 GHz.

49

Figure 25. Cumulative probability of the received power from a corner
reflector as a function of foliage depth; 16.2 GHz.

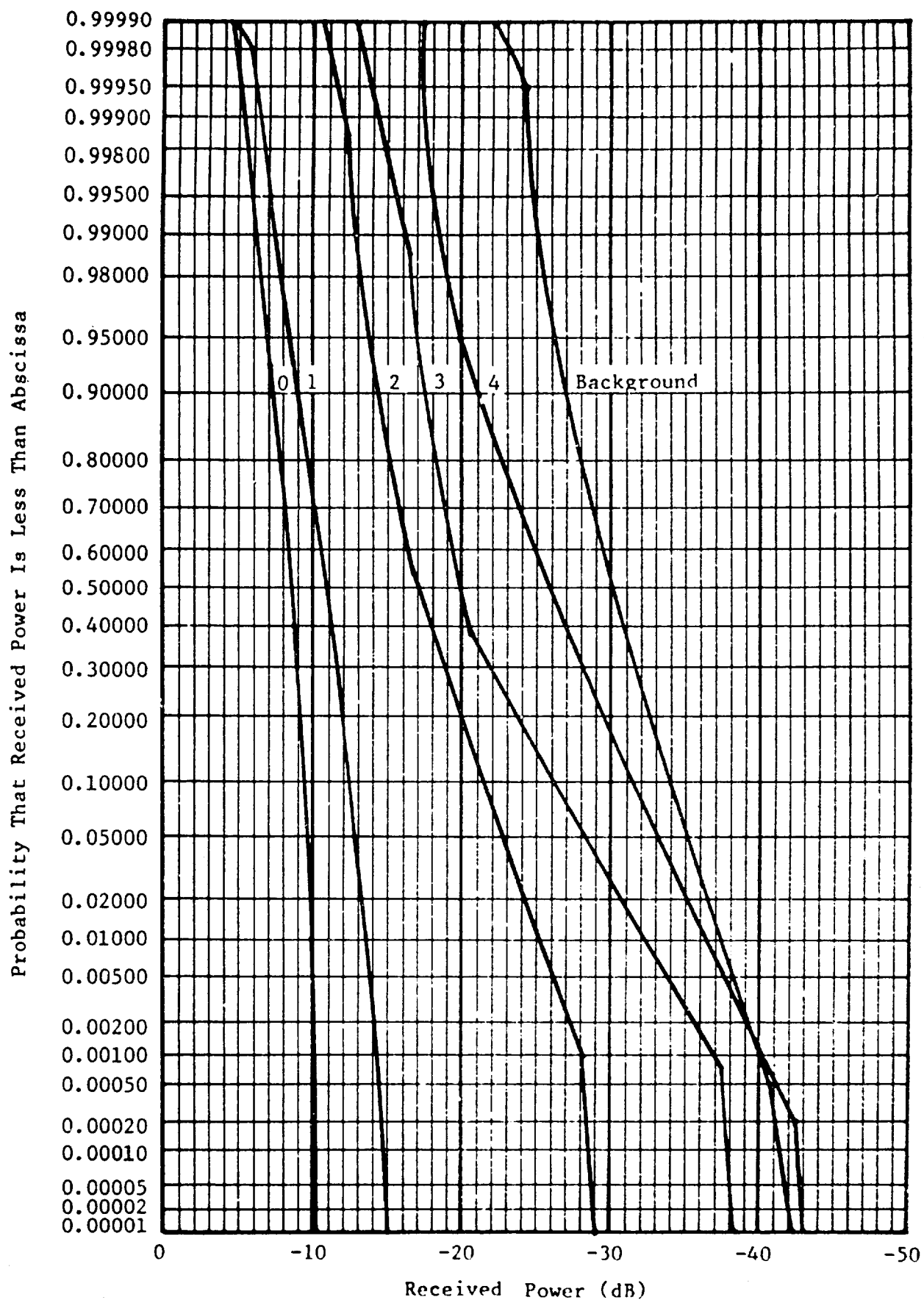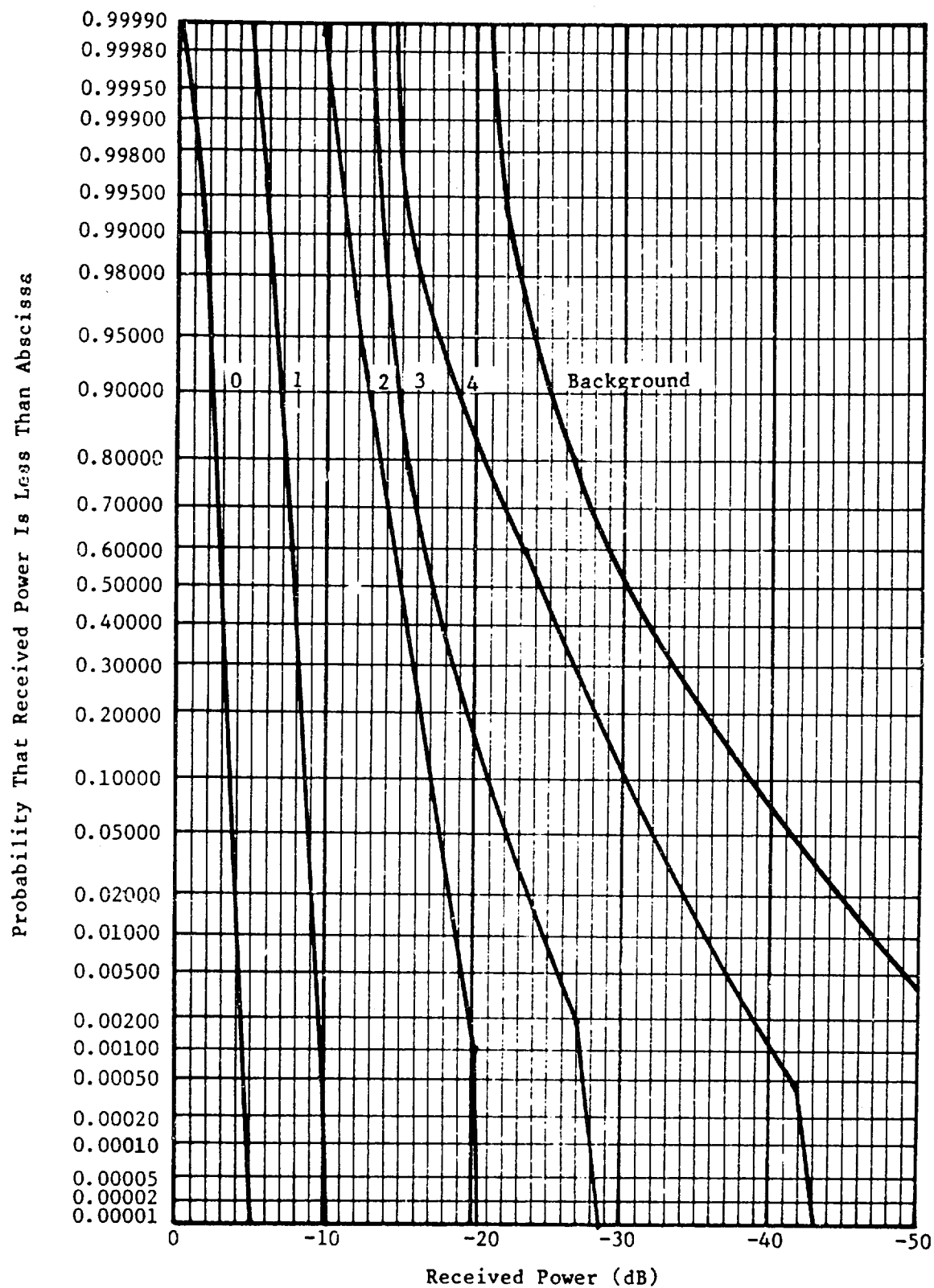Figure 26. Cumulative probability of the received power from a corner reflector as a function of foliage depth; 35 GHz.

Figure 27. Cumulative probability of the received power from a corner reflector as a function of foliage depth; 95 GHz.
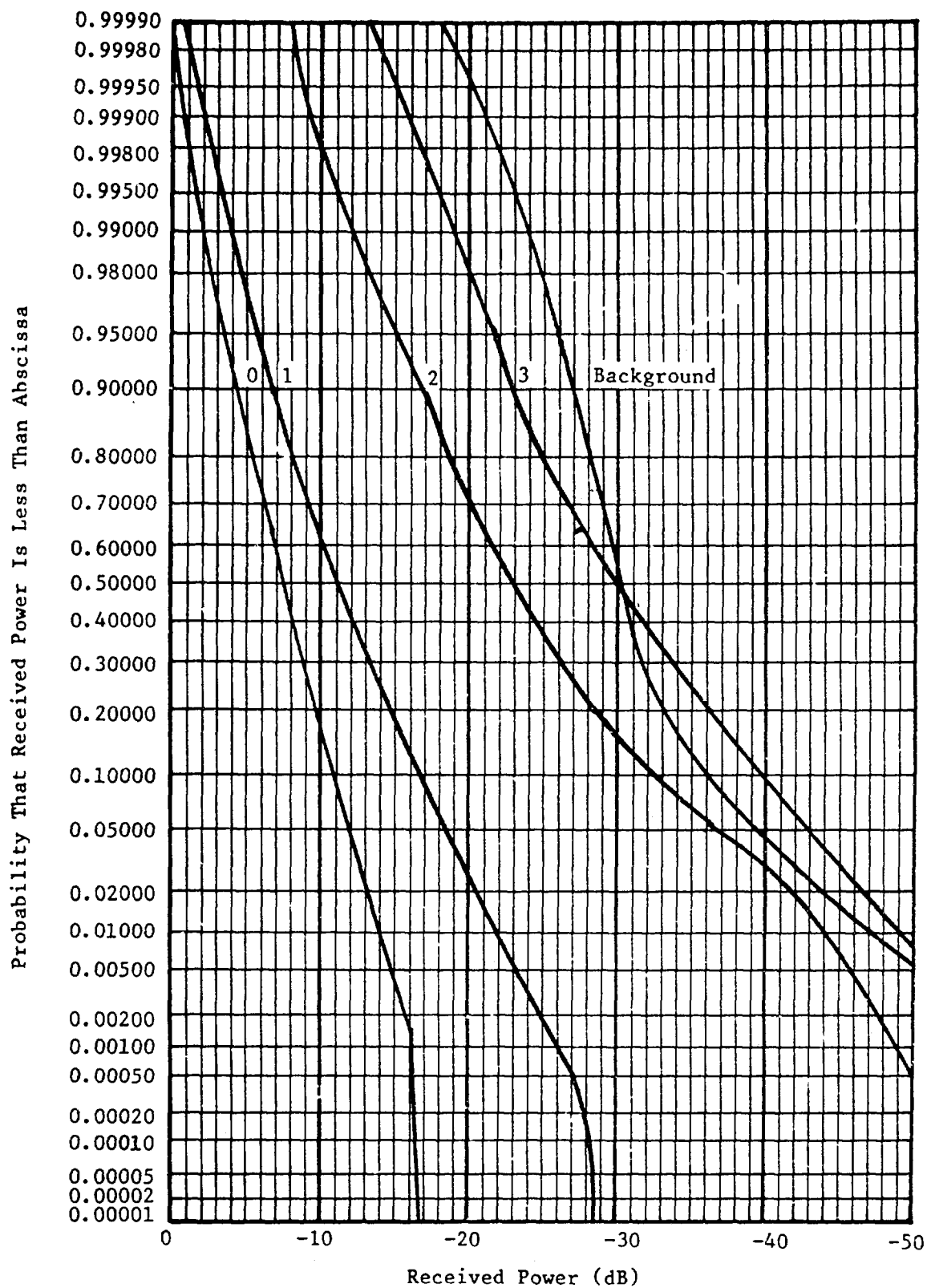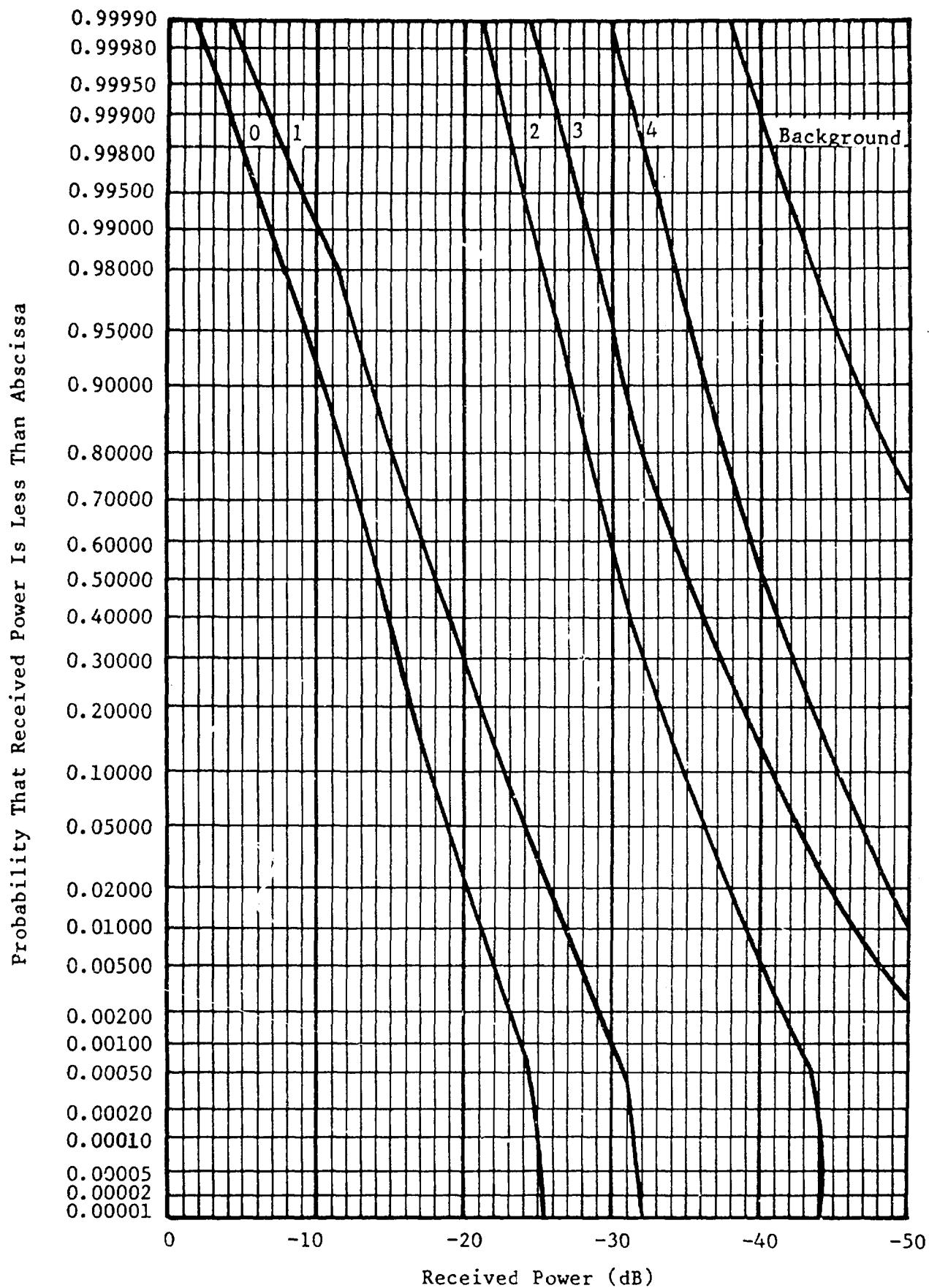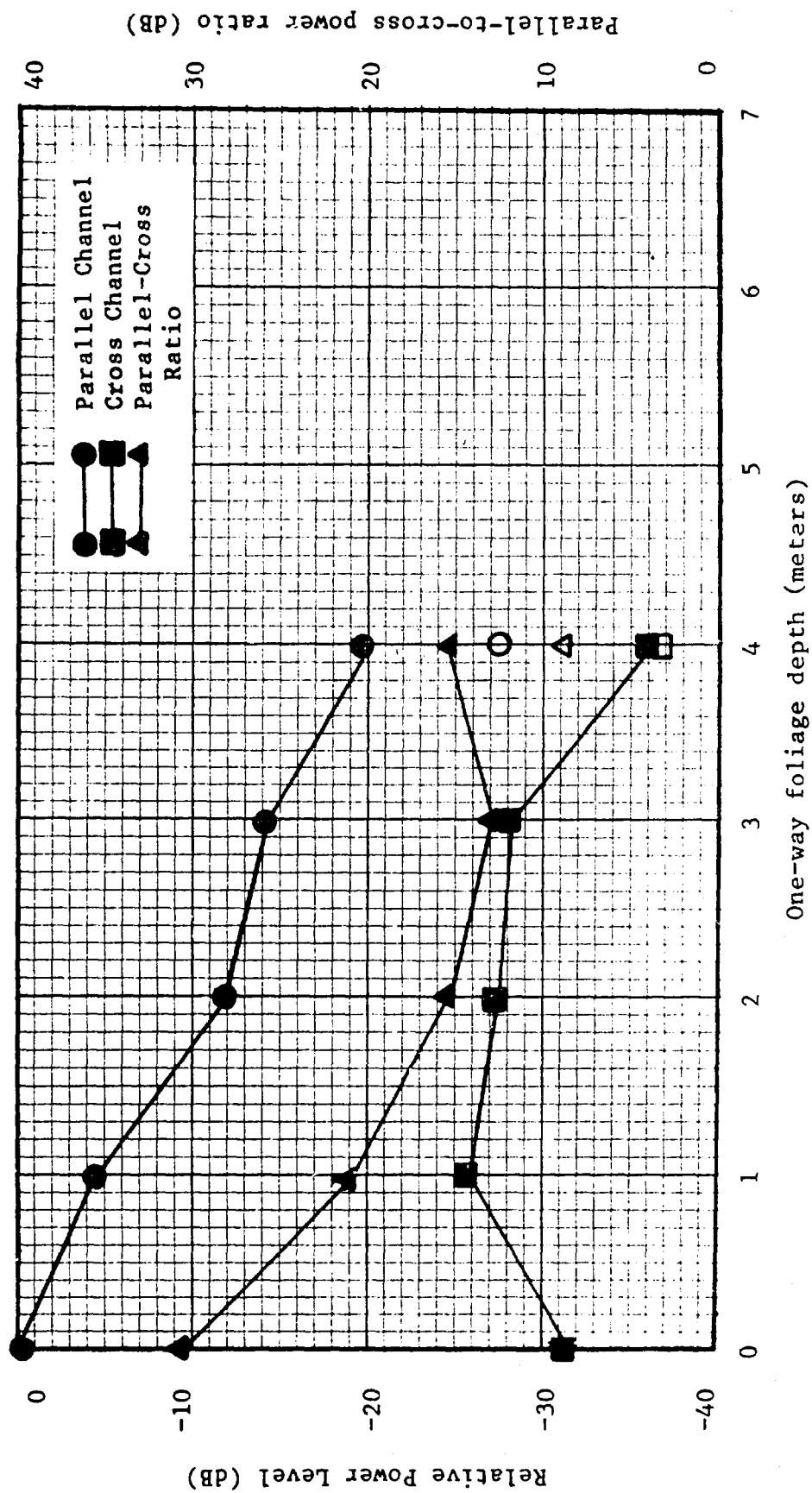
Figure 28. Parallel and cross channel behavior of the return from a 10 inch corner reflector as a function of foliage depth; 35 GHz, vertical polarization. (The open symbols are the background values.)

the clear level, probably due to the depolarization of the signal at the edge of the foliage and then slowly decreases in depth until the background level is reached at 4 meters. The resulting parallel- cross ratio decreases rapidly at the first two meters and then remains approximately constant up to four meters depth. Thus, it can be sen that the parallel-to-cross ratio of the corner reflector decreases rapidly at the foliage edge to about 15 dB and remains approximately constant for the next several meters, whereupon it becomes essentially equal to that of foliage only.

e. Spectral Properties

Examples of the frequency spectra of the signal from a corner reflector as a function of foliage depth are given in Figures 29 and 30 at 35 GHz and 95 GHz. For these runs, the dc term of the Fourier transform was set to zero and the resulting ac components were normalized to the peak value so that the shapes of the distributions could be compared. From the figures, it can be seen that the spectral components of the clear runs are steeper and have a lower cutoff frequency than the runs where the corner is immersed in foliage. Even though the corner is at zero depth, the corner and some trees are both in the same cell of resolution. Thus the total composite return does have a non-zero frequency response. At 3 meters depth, the spectra of the corner is essentially the same as the background spectra. Thus, it would appear to be difficult to discriminate between return from the corner immersed in the foliage and return from the foliage alone using Doppler techniques if the corner were immersed behind two or more feet of foliage, even though the signal from the corner at this depth is 10 dB higher than the background level. Similar results were seen at 9.4 GHz and 16 GHz, but the differences between the cutoff frequency of the clear run and background were much smaller. These results are for noncoherent processing only and care should be taken in extrapolating these conclusions to the coherent Doppler case.
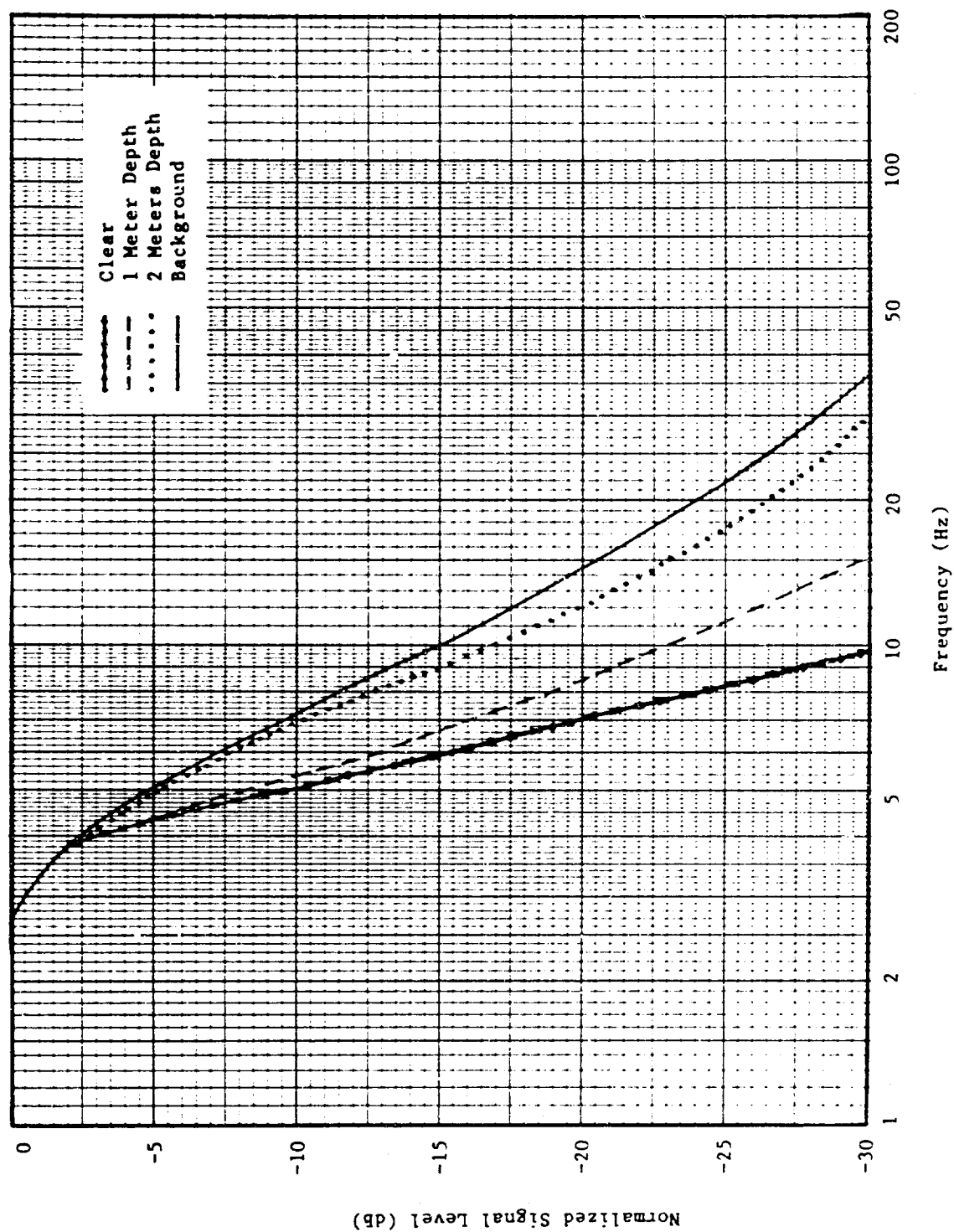
54

Figure 29. Normalized frequency spectrum of the return from a corner reflector at several foliage depths; 35 GHz, 5 mph windspeed.
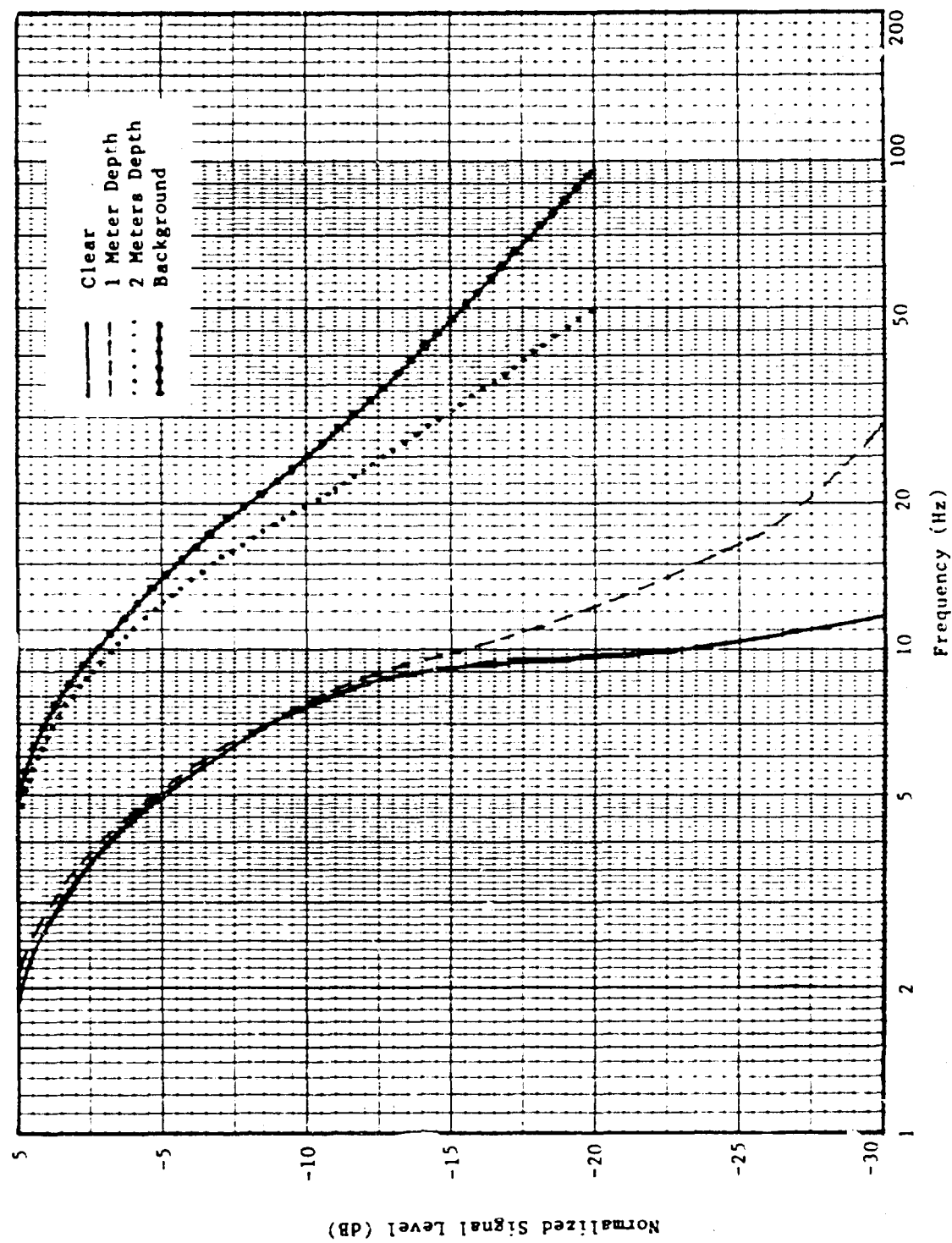
Figure 30. Normalized frequency spectrum of the return from a corner reflector at several foliage depths; 95 GHz, 5 mph windspeed.

III. CONCLUSIONS AND RECOMMENDATIONS

The detailed discussions of the results of the investigations given
in the preceding sections provide a fairly complete review of the experi-
mental program. Unfortunately, only very limited analytical studies and
no theoretical investigations were possible due to the fiscal constraints
on the program. A number of significant conclusions have been determined
and are outlined below.

1. Dry measurements indicate that the attenuation constant varies
    directly with the log of the frequency and is essentially inde-
    pendent of polarization.

2. Wet measurements indicate that the attenuation constant is a power
    function of the log of the frequency.

3. The attenuation constant appears to increase with foliage depth
    particularly at 35 GHz and 95 GHz for both horizontal and vertical
    polarizations.

4. Two-way measurements at 35 GHz and 95 GHz were limited to 4 meters
    foliage depth or less. The apparent increase in attenuation constant
    with foliage depth indicates the possibility of higher average
    values of attenuation for greater foliage depths than those measured.

5. One-way measurements tended to give a higher median value for
    the attenuation constant than the two-way measurements. The
    difference is attributed to differences in illumination functions
    and in foliage depths measured.

6. High-angle measurements gave larger values of attenuation constant
    than the low-angle measurements. The difference is attributed
    to greater density of branches and limbs for the high-angle case.

7. The probability distributions of the received signal from a corner
    reflector show an increased width for an increase in foliage depth.

8. The frequency spectra exhibit an increase in spectral width with
    increasing foliage depth for constant wind speed.

Perhaps one of the most important results of the investigations is
the establishment of a potentially reproducible definition of foliage depth.
The generally used definition of foliage depth appears to be a measure
of total foliage path length based on the line-of-sight distance through
the canopy. Unfortunately this approach requires a detailed description
of the foliage (i.e., type of vegetation, density, etc.) and is not simply

57

reproducible - especially in diverse geographic regions. The proposed definition which was used for the data presented here describes a total foliage depth based on the number of branches in the p th and the size of each branch. This approach shows promise in developing prediction models and in providing a measurements standard, since a surprising degree of similarity in attenuation characteristics apparently exists between foliage types at a branch level.

The current work has really only barely begun the investigation of foliage penetration by the shorter microwave and millimeter wavelengths. A great deal of additional work is needed to provide a comprehensive base for the characterization of the penetration question. A few specific items recommended are given below.

1. One-way penetration measurements should be made for winter foliage conditions, in addition to the two-way measurements currently planned.

2. One-way penetration measurements should be performed for both winter and summer conditions at the higher depression angles.

3. Additional two-way penetration measurements are needed for summer conditions with emphasis on moderate-to-large foliage depths.

4. The matrix of frequencies in the program should be expanded to include L-Band and C-Band measurements.

5. The types of foliage encountered should be expanded by performing measurements at several sites.

6. Future experimental programs should include detailed characterization of the foliage, especially moisture content, leaf thickness and density, as well as more extensive meteorological documentation.

7. Extensive analytical and theoretical investigations should be undertaken to support and guide the experimental measurements.

8. The development of computer algorithms based on the results of the experimental and analytical investigations should be initiated.

58

IV. REFERENCES

1. R. D. Hayes and F. B. Dyer, "Land Clutter Characteristics for Computer Modeling of Fire Control Radar Systems," Technical Report No. 1 on Contract DAAA 25-73-C-0256, Engineering Experiment Station, Georgia Institute of Technology, 15 May 1973.

2. N. C. Currie, F. B. Dyer, and R. D. Hayes, "Analysis of Radar Rain Return at Frequencies of 9.375, 35, 70, and 95 GHz," Technical Report No. 2 on Contract DAAA 25-73-C-0256, Engineering Experiment Station, Georgia Institute of Technology, 1 February 1975.

3. N. C. Currie, F. B. Dyer, and R. D. Hayes, "Radar Land Clutter Measurements at Frequencies of 9.5, 16, 35, and 95 GHz," Technical Report No. 3 on Contract DAAA 25-73-C-0256, Engineering Experiment Station, Georgia Institute of Technology, 2 April 1975.

4. D. E. Wrege and D. S. Harmer, "FOCAL/F An Extended Version of 8-K FOCAL 69 $_{TM}$," School of Nuclear Engineering, Georgia Institute of Technology, 1 June 1972.

5. W. Rivers, "Low-Angle Radar Sea Return at 3mm Wavelength," Final Technical Report on Contract N62269-70-C-0489, Engineering Experiment Station, Georgia Institute of Technology, 15 November 1970.

6. Fred E. Nathanson, Radar Design Principles, McGraw-Hill Book Company, New York, 1969, p. 19.

7. J. A. Saxton and J. A. Lane, "VHF and UHF Reception, Effects of Trees and Other Obstacles," Wireless World, Vol. 61, May 1955, pp 229-232.

APPENDIX A

Foliage Penetration Measurements
Radar Calibration and Operation Procedures

The following procedures were followed in calibrating and operating
the radars and associated instrumentation during the penetration measure-
ments.

I. Preliminary

   a) Start 400 Hz motor-generator set.
   b) Connect 24 volt dc auxiliary supply across 24 volt battery
      supply.
   c) Start 60 Hz motor-generator set.
   d) Disconnect 24 volt auxiliary supply.
   e) Allow speed of both M-G sets to stabilize.
   f) Adjust speed of M-G sets to set frequencies to 60 Hz and
      400 Hz respectively.
   g) Adjust voltages to proper value.
   h) Set up necessary equipment on van roof.
   i) Turn on van power.
   j) Apply power to all radars and test equipment.
   k) Dispatch field crew and equipment to remote location.

II. Calibration Procedures (I-Band, J-Band, K-Band)

   a) Identify tape recorder channels and enter on log sheets.
   b) Turn on transmitters and verify receiver tuning.
   c) Turn off transmitters and set signal generator to transmitter
      frequency.
   d) Calibrate signal generator power levels.
   e) Set range gate to sample peak of calibration signal.
   f) Turn on tape recorder and strip chart recorder.
   g) Each calibration will be preceded with a series of maximum/
      minimum signal levels.
   h) Preset time code generator to correct time.
   i) Start at maximum signal level and reduce signal generator
      level in 10 dB steps until signal is below receiver noise
      level. (Normally a 70 to 80 dB range). Record each level
      for a minimum of 10 seconds and voice label tape with dB
      level and start-stop time.

III. Calibration Procedures. (95 GHz)

   a) Set up a trihedral corner reflector at the previously
      designated clear area.
   b) Set height of corner reflector to maximum and, using appro-
      priate alignment tools, adjust azimuth and elevation to bore-
      sight with the 95 GHz antenna.
   c) Using boresight telescope align 95 GHz antenna with corner
      reflector.

d) Turn on transmitter and verify receiver local oscillator tuning.

e) Set range gate to sample peak of radar return from corner reflector.

f) Starting at maximum signal level increase attenuation in 10 dB steps until signal level is below receiver noise level. (Normally 60 to 70 dB range.) Record each level for a minimum of 10 seconds and voice label tape with dB level and start/stop times.

IV. Data Recording Procedures

a) Refer to remote site procedures.

b) Align each antenna boresite with corner (horn).

c) Activate radar transmitters and adjust range gate to peak of radar return from corner reflector or signal from remote transmitters.

d) Verify that field personnel are ready for data run.

e) Record remote site parameters on log sheets. (location, position, depth, etc.)

f) Start tape recorder and strip chart recorder.

g) Voice label tape with start/stop times, wind speed/direction and other meterological data and mark strip chart with appropriate comments.

h) Record data from each location for a minimum of one minute. (longer if appropriate).

i) End data run and review strip chart to determine if data is reasonable based on previous runs.

j) If data is not consistent with previous history, request field personnel to check for possible remote site effects which would influence data. (Inspect for unusual foliage density, limb blockage, etc., and verify remote equipment pointing angles, power levels, etc.) Enter appropriate information on log sheet.

k) If data limits are reasonable, request field personnel to relocate remote equipment to next position and repeat appropriate items in Section IV of this procedure.

l) At the end of a series of measurements, re-calibrate the radar systems as described in Section II and III of the procedure.

APPENDIX B

Foliage Penetration Measurements
Remote Site Procedures

The following procedures were followed in selecting measurement locations and setting up remote equipment at the Kennesaw Mountain field sites.

1. Visually inspect the location to verify that cultural objects which would interfere with the measurements are not present.

2. Visually inspect the location for adequate foliage density, total penetration depth and height clearance.

3. Locate and mark deepest penetration point.

4. Locate and mark clean reference point on a radial between the radar van and the deepest penetration point.

5. Locate and mark intermediate points along this radial which allow a minimum of 1 meter additional foliage.

6. Measure the total path length between the edge of the foliage and each intermediate position (total penetration path).

7. Measure the foliage depth for each individual contributing branch on tree (total foliage penetration).

8. Count the total number of contributing branches or layers of foliage.

9. Relay all measured data to the radar operator.

10. Set up synchronizing equipment for one-way experiment.

11. Set up either the corner reflector or the remote transmitters and standard gain horns as instructed by radar operator. The reflector (horns) should be positioned directly above clear position marker.

12. For one-way experiments, turn on both I-band and J-band transmitters and adjust magnetron currents to read 1.5 and 3.2 ma respectively. Set horns for vertical or horizontal polarization as instructed by radar operator.

13. The clear data run is the reference to which all other runs in a series are compared to determine attenuation. During all data runs, personnel will clear the area around the measurement site, and notify radar operator when area is clear.

14. After clear data run, change transmitted polarization for cross-channel reference run, and notify radar operator when area is clear. After data run, set polarization as instructed by radar operator.

15. Move remote equipment into foliage area previously selected and notify radar operator when area is clear.

16. At each location, data runs will be made at three lateral positions spaced approximately 1 foot apart. The first run will be on the radial previously selected. Runs 2 and 3 will be 1 foot to the left and one foot to the right of the radial, respectively.

17. For the one-way measurements, 3 vertical runs will be made at each lateral position.

18. Repeat 15, 16, 17 at new locations.

19. After data run at deepest penetration is complete return to clear area for repeat of reference run.

20. Repeat 14 through 19 for the orthogonal polarization.

   NOTE: Items 12, 14 and 17 apply to one-way measurement only.